SYNTHESIS AND CHARACTERIZATION OF FLY ASH BASED SELF-DISPERSING, SELF-SENSING GEOPOLYMER

by

WEI PAN

JIALAI WANG, COMMITTEE CHAIR
AREM AMIRKHANIAN
THANG N. DAO
CHAO ZHAO

A THESIS

Submitted partial fulfillment of the requirements
for the degree of Master of Science
in the Department of Civil Engineering
in the Graduate School of
The University of Alabama

TUSCALOOSA, ALABAMA

2020

ABSTRACT

Extensive studies have been carried out to use carbon nanotubes (CNTs) to reinforce cementitious materials because of the extraordinary strength of CNTs. More importantly, new functions such as self-sensing ability can be introduced to the materials due to the excellent electrical conductivity of CNTs. However, the application of CNTs in reinforcing materials is hampered by three major challenges: proper dispersion of the nanoscale additives, scale-up of laboratory results and implementation on larger scale, and a lowering of the cost benefit ratio. It is not easy to disperse CNTs into cementitious materials.

Aiming to address all these three challenges simultaneously, this study proposes to produce CNTs reinforced cementitious materials through directly growing CNTs on fly ash particles using a novel Poptube method. Unlike any other exiting methods, Poptube method uses microwave irradiation as heating source, and a single chemical (e.g., ferrocene) to provide both the carbon source and the catalyst for CNTs' growth. Compared with existing methods, the Poptube method is much more cost-effective and can be easily scaled-up for mass production.

CNT reinforced geopolymer can be produced by mixing these CNTs grown fly ash particles with other ingredients. In this way, the time-consuming and difficult task of dispersion of CNTs is eliminated since CNTs are self-dispersed into the matrix by the fly ash particles on which CNTs were grown.

To evaluate the effect of growing CNTs on the reactivity of fly ash particles, a series of tests were carried out, including dissolution testing, electric conductivity testing, and imaging with

scanning electron microscopy (SEM) and Atomic Force Microscopy (AFM). Results show that growing CNTs on the surface of fly ash does not reduce the reactivity of the fly ash because of the seeding effect provided by the CNTs.

The composite effect induced by the CNTs was confirmed by Raman Spectrometer, which shows that the D-band of the CNTs varies with the applied thermal stress, suggesting effectively stress transfer from the geopolymer matrix to CNTs. This finding suggests that stress in CNTs reinforced geopolymer can be sensed by a Roman Spectrometer in a non-contact fashion.

The self-sensing function of the nanocomposite mortar is evaluated using a four-electrode-DC method. At early age, geopolymer mortar is piezoresistive because of its high electric conductivity. However, DC induced polarization effect is very serious at this age. This polarization effect reduces with reaction time and becomes negligible at 35d. Similar piezoresitivity was achieved by the geopolymeric nanocomposite produced by using fly ash grown with CNTs using Poptube method, which is three orders magnitude more sensitive than the geopolymer one without any CNTs.

DEDICATION

This thesis is dedicated to everyone who helped me and guided me through countless attempts in finishing this thesis. My parents and close friends who never gave up on me throughout the time.

ACKNOWLEDGEMENTS

I am pleased to have this opportunity to thank many colleagues, friends, faculty and staff members who have helped with this research project.

I would like to express my deep and sincere gratitude to my advisor Dr. Jialai Wang Ph.D., Professor for his patience and encouragement to help me through my study, research, and writing. I would not have the chance to finish this thesis without his help. He taught me the methodology for carrying out the research, and the way to think like a researcher. I would like to thank him for his guidance, kindness, and empathy.

I would like to thank Dr. Mark Barkey for help to set up the period loading test, Dr. Shanlin Pan for the help to set up the Raman spectrum test. I am also grateful for all the committee members for your time and suggestions.

I would like to thank Johnny R. Goodwin for the help for SEM imaging, Rob A. Holler for the help for XRD.

I would like to thank Shinxin Zeng for teaching me how to make geopolymer mortar samples. I also want to show my gratitude to other students in the group for the helps and inspirations. I am thankful to my close friends who never gave up on me and supported me through my life.

Finally, I am extremely grateful to my parents for their love and sacrifices.

CONTENTS

LIST OF TABLES

LIST OF FIGURES

1. INTRODUCTION

1.1 Research Motivation

Portland Cement Concrete (OPC) is foremost among construction materials, which forms the basis of the human society. OPC based concrete demanded nearly three fourth of the existing building and construction materials. World total annual production of OPC is about 4.1 billion metric tons in 2019. 88.5 million Metric tons of OPC was produced in the United States in 2019, and the clinker capacity was 103 million metric tons. [1]

With such magnificent industrial production and demand, any kind of issue and challenge with concrete will be magnified to considerable levels. The current issues and challenges with Portland cement concrete mainly fall into two distinct categories.

First and more recent issue is CO_2 emission. As the number one source of U.S. greenhouse gas emission, carbon dioxide emits 81.3% of all emissions; which, the production of cement claims to be the sixth in the amount of carbon dioxide emission (10.7% of total industrial carbon dioxide emission or 40.3 million metric tons) [2]. The process of the production of Portland cement emitting CO_2 was created by the chemical decomposition of Carbon-containing minerals, for example the chemical decomposition of calcium carbonate providing heat:

$$CaCO_3 \xrightarrow{heat} CaO + CO_2 \quad (1)$$

Each mole of calcium carbonate forms one mole of calcium oxide and one mole of carbon dioxide [2].

Approximately 6% of anthropogenic greenhouse gas emissions in the world is from OPC production [3]. This is an unsustainable energy and CO_2 burden, especially for a material that is manufactured at the scale of more than 4billion tons per year [1]. To improve the eco-efficiency of cement and concrete, the United Nations Environment Program Sustainable Building and Climate Initiative (UNEP-SBCI) has identified three effective approaches: (a) increasing use of supplementary cementitious materials (SCMs); (b) developing sustainable alternative cements; and (c) improving cement efficiency[12]. UNEP-SBCI pointed out that the International Energy Agency's 2050 goal of CO_2 emissions reduction from cement industry by 24% compared to current levels (with an expected increase of 12-23% in global cement production)[12] is too rigorous to be addressed by single approaches.

Secondly, OPC based concretes are susceptible to deterioration when exposed to severe environments. Low tensile strength, high brittleness, and low volume stability make them vulnerable to cracking. Higher permeability, porous microstructure, and thermodynamically unstable chemical compounds such as calcium silicate hydrate (C-S-H) make them susceptible to corrosion and sulfate attack. Deterioration of these OPC-based concretes has emerged as one of the biggest challenges in maintaining and protecting the US infrastructure system. 2017 report card for America's infrastructure received a grade of D+ [4], as grade D+ in 2013. However, the cost to improve has increased from $3.6 trillion to $4.59 trillion [4]. ASCE suggested several key solutions for raising the grades. Two out of the three listed key solutions could be related to the challenges in the cement industry [4]:

"…2. Promote Sustainability and Resilience … 3. Develop and Fund Plans to Maintain and Enhance America's Infrastructure"

One viable strategy to address challenges listed above is finding an alternative of OPC that is greener, has better mechanical property, and has more resilience. Among several of the newly investigated cementitious materials, geopolymer seems to be the best for the current confronting issues and challenges we are facing.

1.2 Geopolymer

A number of new materials, which could replace OPC, have been investigated. These materials include magnesia cement [5, 6, 7, 8], sulfoaluminate cements [9, 10, 11, 12, 13], blended OPC-based cements [14, 15], and geopolymers [16]. Among them, geopolymers are the most promising candidate.

Geopolymers are amorphous three-dimensional alumino-silicate binder materials [16]. They can be synthesized by mixing source material with an alkaline activator and then curing at room or elevated temperature. The source materials based on alumina-silicate should be rich in silicon and aluminum, and could be natural minerals such as clay, kaolinite, or industrial wastes such as fly ash, silica fume, or slag, etc. The alkaline activators are strong chemical bases. Among others, the combination of NaOH and sodium silicate or the combination of KOH and potassium silicate are the most used. Aluminosilicate reactive materials are rapidly dissolved into the strong alkaline solution to form free SiO_4 and AlO_4 tetrahedral units. These SiO_4 and AlO_4 are then polymerized together to form polymeric precursors (–SiO_4 –AlO_4 –, or –SiO_4 –AlO_4 –SiO_4 –, or –SiO_4 –AlO_4 –SiO_4 –SiO_4 –) amorphous geopolymers are produced in the oxygen atoms sharing between two tetrahedral units, and thereby yielding amorphous geopolymers. A hydrated geopolymer has the following empirical formula

$$M_n\{-(SiO_2)_z-AlO_2\}_n.wH_2O \quad (2)$$

where *n* is the degree of polycondensation; *z* is 1, 2 or 3; and M is a cation such as potassium, sodium; and *w* is the number of water molecules in the hydrate [17, 18, 19].

Geopolymers were first introduced by Davidovits in 1972 [16]. A number of names have been used to describe these materials, such as alkaline-activated cements [20, 21, 22], inorganic polymers [23, 24, 25], hydroceramic [26], etc. Geopolymer is the generally accepted name for this technology. Extensive studies have been conducted in the last four decades on geopolymers [27][28]. Kaolinite and calcined kaolinite (metakaolin) were used as source materials in the early and current studies of geopolymers [17, 28, 29, 30, 31]. Industrial wastes such as fly ash [32, 33, 34, 35, 36, 37, 38, 39] and slag [40, 41, 42, 43, 44, 45, 46]are gaining more attentions due to the enormous environmental benefit of using them as source materials.

1.2.1 Green features of geopolymers

Compared with OPC, geopolymers possess following 'green' features besides superior mechanical properties:

a. *Less energy consumption and CO_2 emission during manufacture.* Production of geopolymers consumes 3/5 less energy and creates 80% less CO2 emission than manufacture of OPC [47].
b. *Using industrial wastes, such as fly ash, as source materials.* In 2007, the coal-fueled electric industry generated about 72 million tons of fly ash [48]. Utilization of fly ashes in construction materials creates many environmental benefits, such as conserving landfill space, reducing the depletion of natural resource, reducing energy consumption and CO_2 emission. OPC-based concrete can use fly ash but only 30% can be used in the practice [49]. High-volume fly ash concrete can lift this limit up to 40% [50]. The OPC concrete industry consumes only about 12 million tons of fly each year in America. Fly-ash based geopolymers provide a new solution

to use more fly ash in construction materials.

c. *High durability*. The aluminosilicate binding phase in geopolymers is extremely durable in aggressive environment [51]. Geopolymer concrete and mortars are estimated to have the ability to withstand weathering up to thousands for years without much function loss [52].

d. *Recyclablility*. Recycling construction materials can protect natural resource and eliminate the need for disposal. Geopolymers based concretes are even more suitable for recycling than OPC based concretes as aggregates for new concrete or pavement subbase layers because of their much lower absorption.

The above characteristics position geopolymers as the most promising green materials to replace OPC. Furthermore, geopolymers set very fast, have very high early age strength and good bond with concrete than organic adhesives. These features make geopolymers the ideal candidate to repair/retrofit aging infrastructure. For example, a highway bridge repaired with geopolymers can open to traffic quicker than that repaired with OPC. Fiber reinforced composites with organic polymer matrix have been used to repair/strengthen reinforced concrete structures [53, 54, 55, 56]. There two major concerns about this technique, long-term durability and fire resistance [57, 58, 59, 60], which prevent wide-adoption of this technique. These two concerns can be eliminated if the organic polymer matrix is replaced by geopolymers because geopolymers have better bonding with concrete and high resistance to degradation due to moisture, ultraviolet lights, and fire hazards [58, 59, 60].

From a sustainable perspective, many other common materials, such as organic plastics, steel and aluminum, ceramics, should also be replaced by more sustainable materials such as geopolymers because the manufacturing processes of these materials are energy intense and starting materials are quite expensive. However, two inherent drawbacks of geopolymers,

brittleness and low tensile strength, restrict their applications as structural materials in place of organic plastics and metals. Compared with that of organic polymers, the toughness and strain at failure of geopolymers is 1000, and 65 times lower, respectively [61]. Due to high brittleness, their failures are catastrophic. These drawbacks have been shown in fiber-reinforced geopolymer composite [61]. With very low strain capacity, geopolymer resins tend to crack at small load before tensile stress can be effectively transferred to fibers. When used to strengthen concrete beam, they rupture first, leading to premature failure of the strengthening [61].

The production of geopolymer requires a source material and a liquid phase. The source material must contain high concentration of silicon and aluminum. Examples of this kind of material are fly ash, metakaolin, kaolinite, clay, garnet, etc. The thesis focusses specifically on fly ash-based geopolymer.

Fly ash is one of the coal combustion products produced mostly, in the United States, by coal power stations. It is a composition of fine particles captured by particle filtration before gas enters the chimney. Fly ash is classified into 2 types, class F and class C, based on their percentage of lime (CaO) content. Class C fly ash contains more than 10% of lime, such high content makes this type of fly ash not suitable for making geopolymer due to fast setting. Class F fly ash contains less than 10% of lime, this is the type used in the experiences performed by the author and analyzed in this thesis. The chemical composition for the two types of fly ash is shown in Table 1.

Table 1. Chemical compositions of Class F and C fly ashes

	Class F (%)	Class C (%)
SiO_2	47.2 – 54	18 - 24.8
Al_2O_3	27.7 – 34.9	12.1 – 14.9
Fe_2O_3	3.6 – 11.5	6.3 – 7.8
CaO	1.3 – 4.1	13.9 – 49
Free lime content	0.1	18 - 25
MgO	1.4 – 2.5	1.9 – 2.8
SO_3	0.1 – 0.9	5.5 – 9.1
Na_2O	0.2 – 1.6	0.5 – 2
K_2O	0.7 – 5.7	1 - 3

Fly ash particles are mostly glassy hollowed spheres with size from 1 to 200 μm. Variations of size, shape, texture, and surface coating depends on the source of coal and the combustion environment [62]. Fly ash can also be synthesized into 15 different zeolites in NaOH or KOH solutions by varying the temperature and duration [63].

A study by Sindhunata et al. (2006) showed the addition of soluble silicate can increase the degree of geopolymerization [64]. Based on this study, waterglass was added to the mixture, as a source of soluble silicate, to increase the degree of geopolymerization.

In order to obtain samples with appropriate compressive strength, the amount of fly ash particles dissolved must be kept high. Therefore, based on the study of Kumar et al (2005), a high concentration of sodium hydroxide is required [65]. 10M in concentration of NaOH is used in the experiments during this study.

1.2.2 Carbon nanotubes

To extend the applications of geopolymers, their tensile strength and toughness must be enhanced. One feasible approach to reach this goal is to reinforce and toughen geopolymers

using carbon nanotubes. Carbon nanotubes (CNTs) are graphitic sheets seamlessly rolled into tubular structures, with diameters ranging from nanometer to tens of nanometers, and lengths up to centimeters. They can be looked at as single molecules, regarding their small size (~nm in diameter and ~ um length), or as quasi-one-dimensional crystals with translational periodicity along the tube axis. The diameter and microscopic structure of the tubes depend on how a sheet is rolled into a cylinder. These are defined by the chiral angle, the angle of the hexagon helix around the tube axis. In macro scale, carbon nanotubes exhibit properties from its homogeneous cylindrical structure; in micro scale, its properties come from the microstructure of the tubes. The latter include, for instance, the electronic band structure their metallic or semiconducting nature. The complex microscopic structure with tens to hundreds of atoms in the unit cell can be described in a very general way with the help of the nanotube symmetry. This greatly simplifies calculating and understanding physical properties like optical absorption, phonon eigenvectors, and electron-phonon coupling.

A tube made of a single graphite layer rolled up into a hollow cylinder is called a single-walled nanotube (SWNT); a tube comprising several, concentrically arranged cylinders is referred to as a multiwall tube (MWNT). Single walled tubes form hexagonal-packed bundles during the growth process. The distance between two tubes, and graphite interlay distance is in the same range. Multiwall nanotubes has a much wider diameter, but similar lengths as single-walled carbon nanotubes. Their inner diameter is around 5 nanometers and outer diameter is around 100 nanometers. Many of the properties of multiwall tubes are already quite close to graphite. While the multiwall nanotubes have a wide range of application, they are less well defined from their structural and hence electronic properties due to the vast possible number of layers.

1.2.3 CNT-reinforced nanocomposite

CNTs have extraordinary mechanical properties, such as strength (tensile strength > 100 GPa), stiffness (Young's modulus of ~ 1.5 TPa), flexibility (20%-30% at failure) [66, 67, 68, 69, 70, 71, 72, 73], making CNTs ideal candidate to reinforce and toughen composite materials to produce nanocomposites. In addition to enhanced mechanical properties, the resulted nanocomposites also possess many non-load-bearing functions, eliminating the need of add-on attachments and penalty of additional weight. Two important functions of structural materials enhanced by CNTs are electrical and thermal conductivities.

Electrical conductivity is critical for composites to survive environmental effects like electrical storms, and also provides an important self-sensing capacity to the nanocomposites. Once CNTs are added into the material, dispersed CNTs are able to form a conductive percolating network in the matrix making the matrix more electrically conductive. Experimental studies have shown that this electrical conductivity of CNT reinforced nanocomposites also varies in proportion with the stress/strain, suggesting that CNT reinforced nanocomposites can sense their own straining [74, 75]. Thostenson and Chou [76, 77] also demonstrated that CNTs reinforced composites can sense the damage in the composite. This is because damage in the composite, which usually starts from a micro-crack in the matrix, can break the conducting pathways in the percolating of the CNT network. As a result, a significant change of electrical conductivity can be observed after the damage occurs. This self-sensing of strain/damage ability of CNT reinforced composites is of great importance to the health monitoring of structures.

Similar to electrical conductivity, ding CNTs with high thermal conductivity into the matrix can significantly increase the thermal conductivity of the composite, leading to wider applications of nanocomposite in thermal management.

1.2.4 Challenges of CNT reinforcement

CNTs, as known as carbon nanofibers (CNFs) have been used to reinforce OPC [78, 79, 80, 81, 82, 83, 84, 85, 86, 87]. However, the application of CNTs in reinforcing materials is hampered by three major challenges [88]: "proper dispersion of the nanoscale additives, scale-up of laboratory results and implementation on larger scale, and a lowering of the cost benefit ratio." Due to strong van der Waals forces between CNTs, CNTs are easy to conglomerate to form bundles and ropes [89]. It has been shown that poor dispersion and rope-like entanglement of CNTs can weaken composites significantly [90]. For this reason, results on CNTs reinforcing reported are not consistent [91, 92, 93, 94].

A homogeneous dispersion of CNTs into matrix is the key to reach ideal reinforcing effect [89]. Using traditional compounding technique is difficult to reach good dispersion. Figure 1 shows poor dispersion of CNFs by only using mechanical mixing [86].

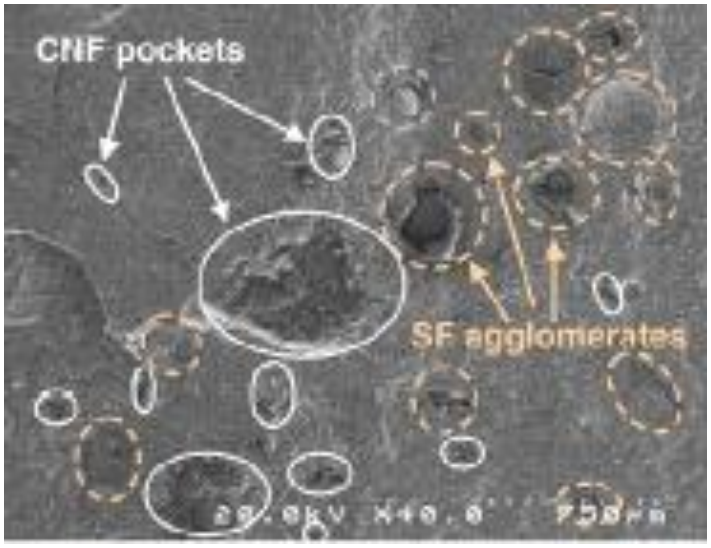

Figure 1. SEM image showing poor dispersion of CNT/Fs in OPC matrix [86]

A few techniques have been commonly used to improve the dispersion of CNTs in matrix, including optimal physical bleeding, in-situ polymization, and chemical functionization [89]. Shah et al. [78] shows that CNTs can strongly reinforce the OPC matrix at the nanoscale once good dispersion of CNTs is obtained. Recently, a more promising approach has been proposed to disperse CNTs in the matrix [95]. Instead of dispersing CNTs into cement matrix, Nasibulin et al. grew CNTs directly on the surfaces of cement particles. After homogeneously mixing these cement particles into cement mixture, those CNTs are naturally dispersed into the cement matrix. In this way, the time-consuming and difficult task of dispersion of CNTs is eliminated. A 100% increase in compressive strength has been obtained for the cement paste reinforced in this manner [95]; while only 30% increase in compressive strength has been obtained by using other dispersion methods. This indicates that this new approach may be more effective than other existing dispersion methods.

Compared with materials used in other areas, civil infrastructural materials are usually used in a much larger volume. Reinforcing bulky construction materials require large amounts of

CNTs, even at a very low loading fraction. The high demand of CNTs poses two challenges [88]: 1) scaling up the current laboratory-size manufacture of CNTs to provide sufficient supply, and 2) lowering the cost of CNTs.

1.3 Innovation: PopTube Method

Aiming to address all these three challenges simultaneously, this study proposes to produce CNTs reinforced cementitious materials through directly growing CNTs on cement particles using Poptube method [96]. The time-consuming and difficult task of dispersion of CNTs can be eliminated by this method since CNTs are self-dispersed into the matrix by the cement particles on which they were grown. Current synthetic approaches to micro- and nano-sized carbon fibers, where pitch-based precursors [95, 97] or carbon-containing gases were involved, frequently require high temperatures for extended periods of time. For the synthesis of tubular structured nanocarbons, since the use of inorganic templates is needed, the subsequent removal steps become necessary [98, 99]. As a result, CNTs manufactured through these approaches are expensive, and unsuitable for applications in construction materials, where large volume of the material is usually needed. Unlike any other exiting methods, Poptube method uses microwave irradiation as heating source, and a single chemical (e.g., ferrocene) to provide both the carbon source and the catalyst for CNTs' growth. Compared with existing methods, the Poptube method is much more cost-effective and can be easily scaled-up for mass production.

Three steps are needed to grow CNTs on micro particles (fly ash) using the this method (Figure 2): i) a layer of conducting polymer is in-situ deposited on the surface of the particles during the polymerization reaction, which takes only about 30 minutes to complete, and the quantities of the products can easily reach 100 gram to kilogram level with simple bench top reactions in the lab scale; ii) the resultant particles with conducting polymer coatings will be

mixed well with ferrocene in solid state; and iii) upon microwave irradiation, the temperature of the conducting layer will rise rapidly as it absorbs the irradiation, the raised temperature will decompose ferrocene into iron and cyclopentadienyl groups. On this stage, carbon nanotubes will be formed with iron nanoparticles stuck on the surface of the conducting layer as the catalyst, and pyrolyzed carbon atoms from the cyclopentadienyl ligand as the source.

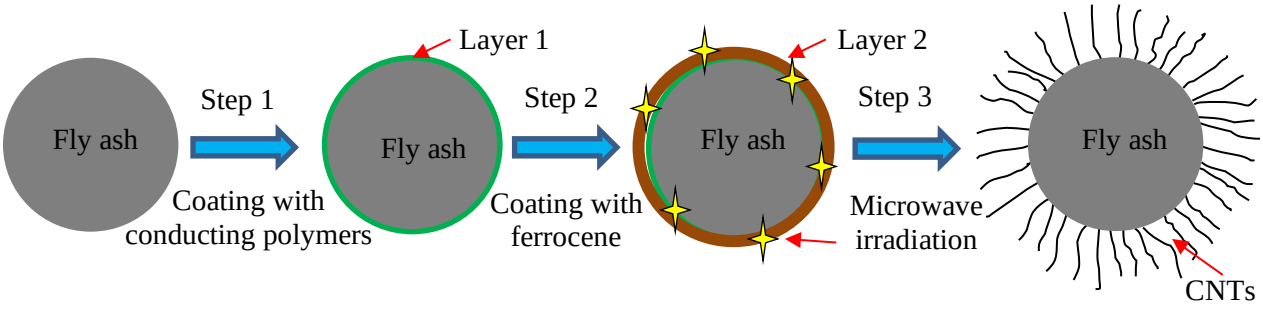

Figure 2. two-layer, three-step approach to grow CNTs on the surface of fly ash

Using this method, it takes only 15-30 seconds to grow CNTs on fly ash particles at room temperature in the air (Figure 3 (a)). In addition, it makes the requirements of Chemical Vapor Deposition (CVD) approach – stock gases feeding, and inert gas protection – unnecessary. High resolution transmission electron microscopy (TEM) image (Figure 3(b)) shows that the CNT manufactured by this method is mainly multi-walled nanotubes (MWNT) in nature, with around 20 layers of coaxial carbon lattice. It also shows that some of the catalyst nanoparticles are at the tip or middle part of the CNTs, indicating that those CNTs are in the tip-growth mode (Figure 3(c)) instead of base-growth mode [96].

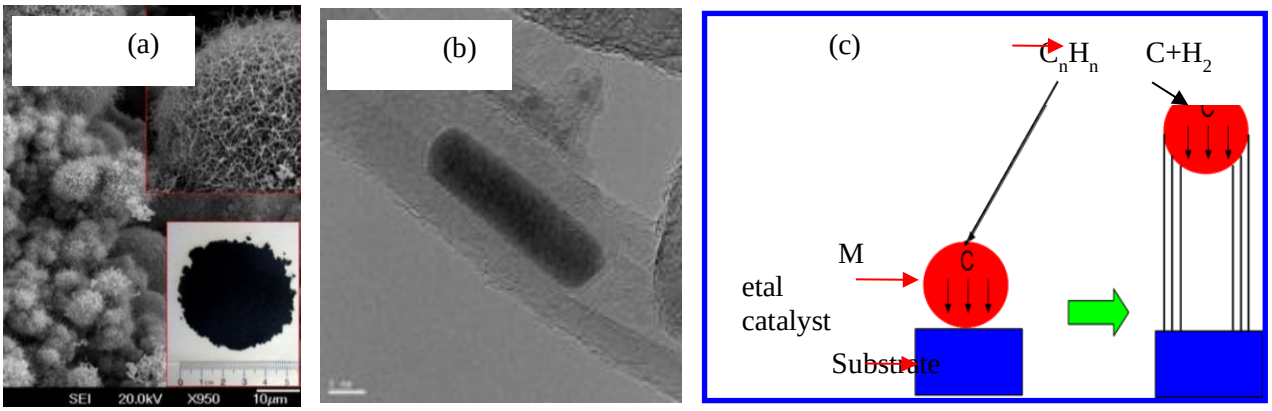

Figure 3. CNTs grown on fly ash particles using microwave heating: (a) SEM images of as produced CNTs on fly ash; (b) TEM image of as-produced CNTs; (c) Tip-growth mechanism of CNTs

1.4 Research Objectives

The major objective of this study is to demonstrate that self-dispersing, self-sensing, CNTs reinforced nanocomposite can be synthesized using the Poptube method. To this end, a fly ash-based geopolymer is chosen as the matrix. The effect of CNTs grown on the surface on the reactivity of fly ash was first evaluated. A series of experiments were carried out to characterize the produced mortar samples with nanocomposite as the binder. In particular, Raman spectra were used to evaluate the stress transfer between the CNTs and the geopolymer matrix. Finally, the self-sensing function of the mortar sample was experimentally demonstrated.

2. EFFECT OF CNTS GROWN ON THE SURFACE ON THE REACTIVITY OF FLY ASH

2.1 Introduction

Poptube method requires coating conductive polymer and precursor of CNTs on the surface of the fly ash. Although most of these coating materials will be consumed during the CNT growth process, it is inevitable to have some residue attached to the surface of the fly ash. This residue together with CNTs on the surface of the fly ash reduces the reaction surface available for geopolymerization, leading to lower reactivity. Therefore, the primary objective of this task is to evaluate the reactivity of the fly ash before and after growing CNTs with Poptube method.

2.2 Materials and Methods

2.2.1 Fly ash

Low-calcium fly ash from Gaston, Alabama, United States, was used to synthesize the geopolymer. Its chemical composition, physical properties and particle size distribution are shown in Table 1, Table 2, and Figure 4, respectively.

Table 2. Physical properties of the fly ash

Properties	Specific gravity	Fineness (% retained on #325 sieve	Mean size (μm)	Mid-size (μm)
Value	2.33	17.23	3.43	2.24

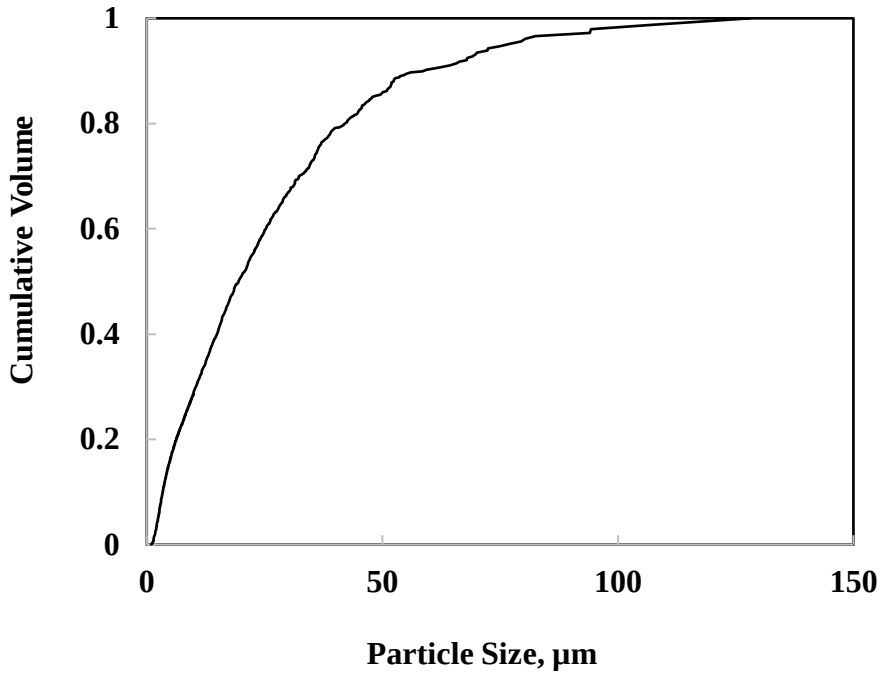

Figure 4. Particle size distribution of the fly ash

2.2.2 In-situ growing CNTs on fly ash particles using Poptube method

Fly ash particles were first dispersed in 1 M aq. HCl under magnetic stirring for 10 min. Second, Pyrrole (0.24 M) was added into the dispersed fly ash/HCl mixture suspension, stirring for another 10 min. Then 0.03 M ammonium peroxydisulfate (APS) was added into the solution mixture and continued stirring for 4 h resulting in polypyrrole (PPy) coated fly ash in the form of dark precipitates. The resulting black precipitate of PPy coated fly ash was suction filtered, washed with copious amounts of aq. 1 M HCl and acetone and finally freeze dried for 12 h. The produced PPy coated fly ash was blended with ferrocene in a plastic vial and spun in a speed mixer at 3500 rpm for 5 min. Then the blend was placed in a glass vial and heated under microwave irradiation for 15 -30 sec. to grow CNTs. Scanning Electron Microscope (SEM) and

Transmission Electron Microscope (TEM) were used to examine whether CNTs were successfully grown on fly ash particles.

2.2.3 Dissolution testing of the fly ash particles with and without CNTs

Dissolution testing was carried out to estimate how much chemical compositions in the fly ash before and after growing CNTs can be dissolved in the alkaline activator. This was carried out by dissolving about 1.5 g of fly ash samples in 156 g 10M NaOH solution, which was used to manufacture the geopolymer matrix in this study. Five samples were tested for both plain fly ash and fly ash grown with CNTs following the procedure described in details in our previous study [100]. The dissolution degree is defined as the mass ratio in percentage between the materials dissolved in the NaOH solution and the total mass of the original fly ashes. Higher dissolution degree means more materials in fly ash can be dissolved by NaOH to participate into the geopolymerization and to produce more geopolymer gel.

2.2.4 Electrical conductivity testing of fly ash suspension in alkaline solution

As demonstrated in our previous study [100], dissolution testing is not sufficient to measure the reactivity of fly ash. Therefore, electrical conductivity testing of fly ash suspension before and after growing CNTs in alkaline solution was carried out to provide another way to peek into the effect of growing of CNTs on the reactivity of the fly ash. Electrical conductivity testing was used to determine the pozzolanic activity of mineral additions such as fly ash [101] because of its simplicity.

Unlike used in OPC based binder in which conductivity testing is carried out in the suspension of fly ash in the calcium hydroxide solution, fly ash used in geopolymer is activated by alkaline activator. Therefore, conductivity testing of fly ash particles with and without CNTs

was carried out in the suspension with sodium hydroxide solution. Since fly ash has water soluble salts which can contribute to the conductivity of the suspension, the conductivity of fly ash suspension in deionized water was measured first. To this end, a suspension of 6 g of fly ash particles in 200ml of deionized water was made and stirred at a rate of 300 rpm using a magnetic stirrer. A conductivity meter was used to measure the conductivity of the suspension until the reading is stable. After that, same amount of fly ash was added to 0.05M NaOH solution to create a new suspension. The conductivity of this new suspension varying with time was then recorded. Although much higher concentration (14M) of NaOH solution was used in synthesizing geopolymer, it cannot be used for conductivity testing because the high concentration of ions produced by 14M NaOH solution can overshadow any change of conductivity induced by the fly ash. The difference between the conductivity measured in the suspension with NaOH solution and in the one with deionized water gives the electric conductivity of the suspension due to the dissolution and reaction of fly ash with NaOH. Conductivity tests were conducted at ambient temperature (23°C), as well as an elevated temperature (40°C) to understand the effect of high temperature curing. To do this, the set-up is moved into an oven, as shown in the testing set-up (Figure 5)

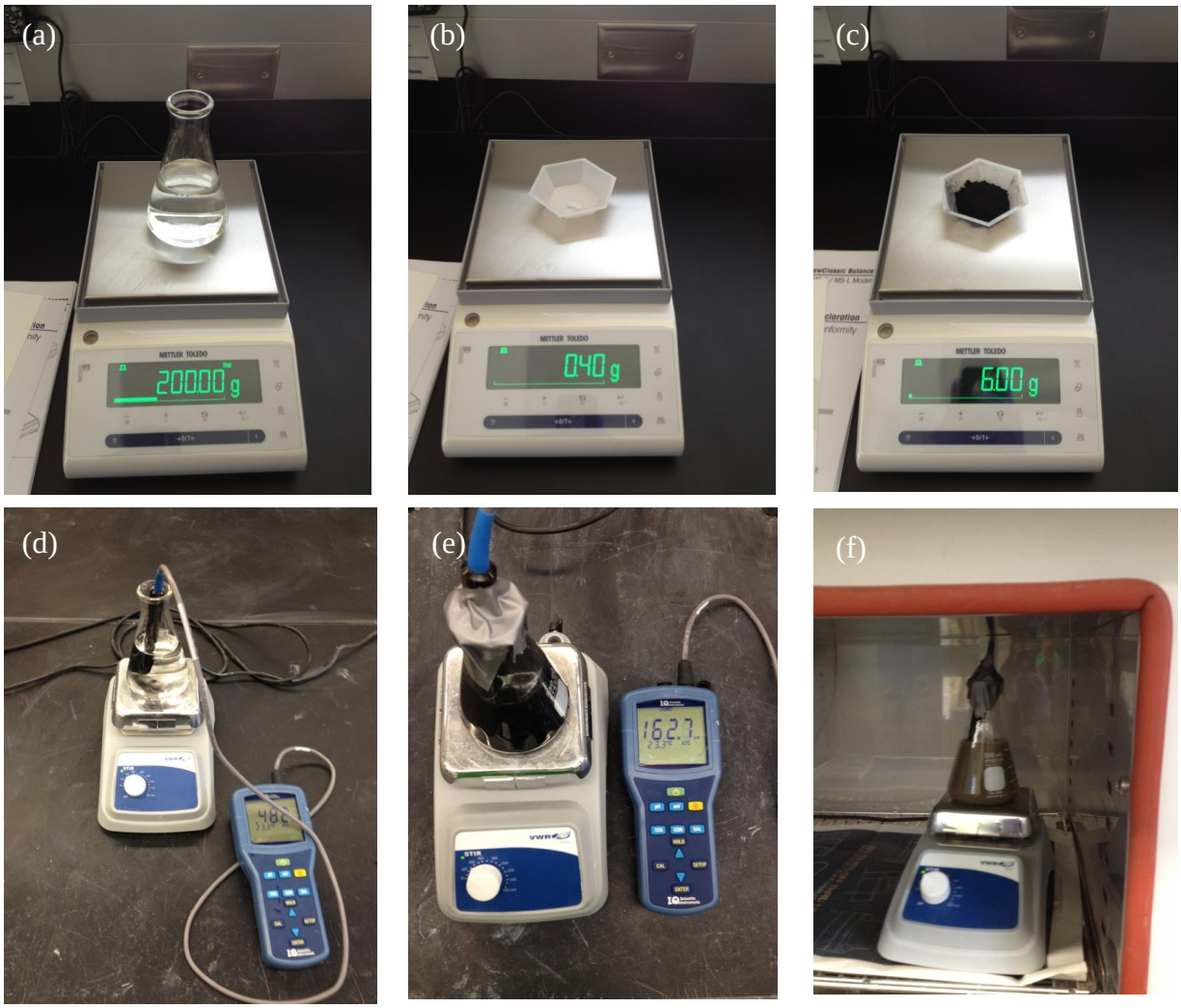

Figure 5. Conductivity test set-up: (a) Weigh water; (b) Weigh NaOH; (c) Weigh fly ash; (d) Water test; (e) Room temperature test; (f) 40 ℃ test

2.2.5 Directly observing dissolution of fly ash without/with CNTs in strong alkaline solution using Scanning Electron Microscope (SEM) and Atomic Force Microscopy (AFM)

To understand the possible difference shown between the dissolution testing and the conductivity testing, SEM and AFM were used to directly observe the effect of growing CNTs on the geopolymerization process on a single fly ash particle.

Scanning Electron Microscope (SEM) uses electron beams to scan a sample and produces images, topography, and composition. The resolution of SEM can provide detailed texture of an object as small as 1 nanometer. Various types of electron detector can be chosen to detect the signals generated. The secondary electron detector was mainly used in the following tests.

The SEM's at the Central Analytical Facility at the University of Alabama were Philips XL 30 SEM and JOEL 7000 FE SEM. Both SEM requires a dry sample therefore no in-situ tests could be monitored using the systems. An alternative way is to treat the sample as it is in the same environment of forming geopolymer for different length of time and perform several different tests using the same sample with those different treatment lengths respectively.

To this end, we impregnated fly ash particles into epoxy matrix to make fly ash-epoxy composite. We mixed 33% Gaston class F fly ash with 67% Tyfo® TC epoxy. The epoxy was prepared by mixing the epoxy and 23% hardener by weight. It was then mixed with the weighted fly ash. The mixture was then flattened by pressing another weigh boat onto the one containing the mixture. The mixture then was given 48 hours to cure. After curing, the specimen was grounded (p4000 size sandpaper) to obtain an even, smooth and flat surface. Another purpose of the grinding is to cut-open some of the fly ash particles for monitoring the reaction inside. After the grinding, the specimen was cut into small sizes to fit into SEM. Figure 6) shows a picture of the cut-and-marked specimens.

The Atomic Force Microscope is an ultra-accurate tool for imaging samples at size of nanometers. Not only that, it forms three dimensional images. This function of AFM makes it a better tool for analyzing structural changes on samples-over-geopolymerization than the SEM. The SEM requires coating on samples with a porous structure. Therefore, monitoring sample-over-geopolymerization is very difficult to accomplish. More importantly, the sample must be

dried and vacuumed, making it not possible to observe the on-going geopolymerization process using SEM. Therefore, AFM was used to in-situ examine the early stage reaction of fly ash in alkaline solution.

An Electrostatic Force Microscopy (EFM) type of AFM was used in this study. In this AFM, a conductive tip is electrically biased against a grounded sample and the derivative of the electrostatic force is probed. The contact potential difference and the height information can be obtained simultaneously. Therefore, EFM can be used to obtain both the morphology and the local electrostatic properties of geopolymer.

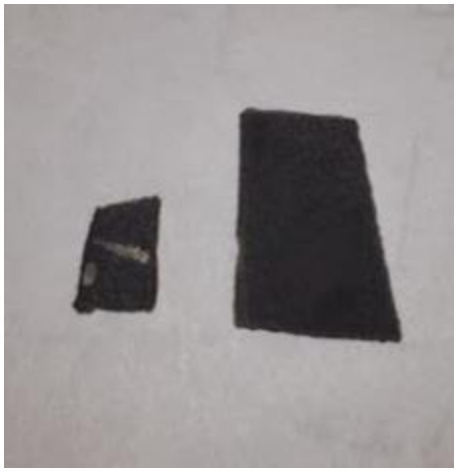

Figure 6. Fly ash – epoxy mixture specimen used for AFM and SEM respectively (left to right)

First, a set of images were taken by both AFM and SEM to allocate several fly ash particles that are easy to identify over the entire test. Some of those are in their original shape, others are cut in half by the grinding process. Therefore, it is possible to monitor reactions both on the surface and inside the particles. For SEM imaging, particles are allocated by the unique crack shapes along the edges of the specimen. For AFM analysis, applying a thin line of silver paste on the monitoring surface of the specimen helps the allocation of the particles by recognizing the

unique shapes of the particle and the edge of the silver paste. The images are also used for a comparison of between the treated and untreated specimens for the purpose of this test.

Second, the specimens are treated in NaOH solution with fixed concentration. For this treatment, the specimen was sunk into 10M NaOH solution and stirred at a rate of 600 rpm using a magnetic stirrer for desired treatment duration. To ensure the consistency of the research, this concentration matches the solution used as alkali activator for specimens made for compression tests. The fly ash particle from Gaston power plant was inspected for four different length of treatment time: before treatment, 2 hours of treatment, 10 hours of treatment, and 24 hours of treatment.

2.3 Results and Discussion

2.3.1 Growing CNTs on fly ash particles using the Poptube method

Results of in-situ growing CNTs on fly ash using the Potpbute method is shown in Fig. 5. Figure 7(a) shows the SEM image of the fly ash particles used in this study. Figure 7(b) shows the image of fly ash particles coated with PPy. Figure 7(c) shows that CNTs have been successfully grown on the fly ash particle using the Poptube method. Figure 7(d) shows the TEM images of some nanocarbons in Figure 7(c), which suggests that hollow nanocarbons (CNT) were produced, possessing outer diameter in the range of 30-50 nm, and with catalyst nanoparticles trapped in the tubular structures.

Fig.5 shows that the quality of CNTs are not as good as those produced by traditional method such as chemical vapor deposition method. This is because the ultrafast growing process of CNTs in the Poptube method. In addition to CNTs, some residual of the precursor can be found. For large-scale application in construction materials such as concrete, the low cost and high productivity are two critical features. Poptube method possesses these salient features at the

expense of the quality of the produced CNTs. Those fly ash particles grown with CNTs were used to manufacture geopolymeric nanocomposite without further purifying to keep the cost acceptable for real applications.

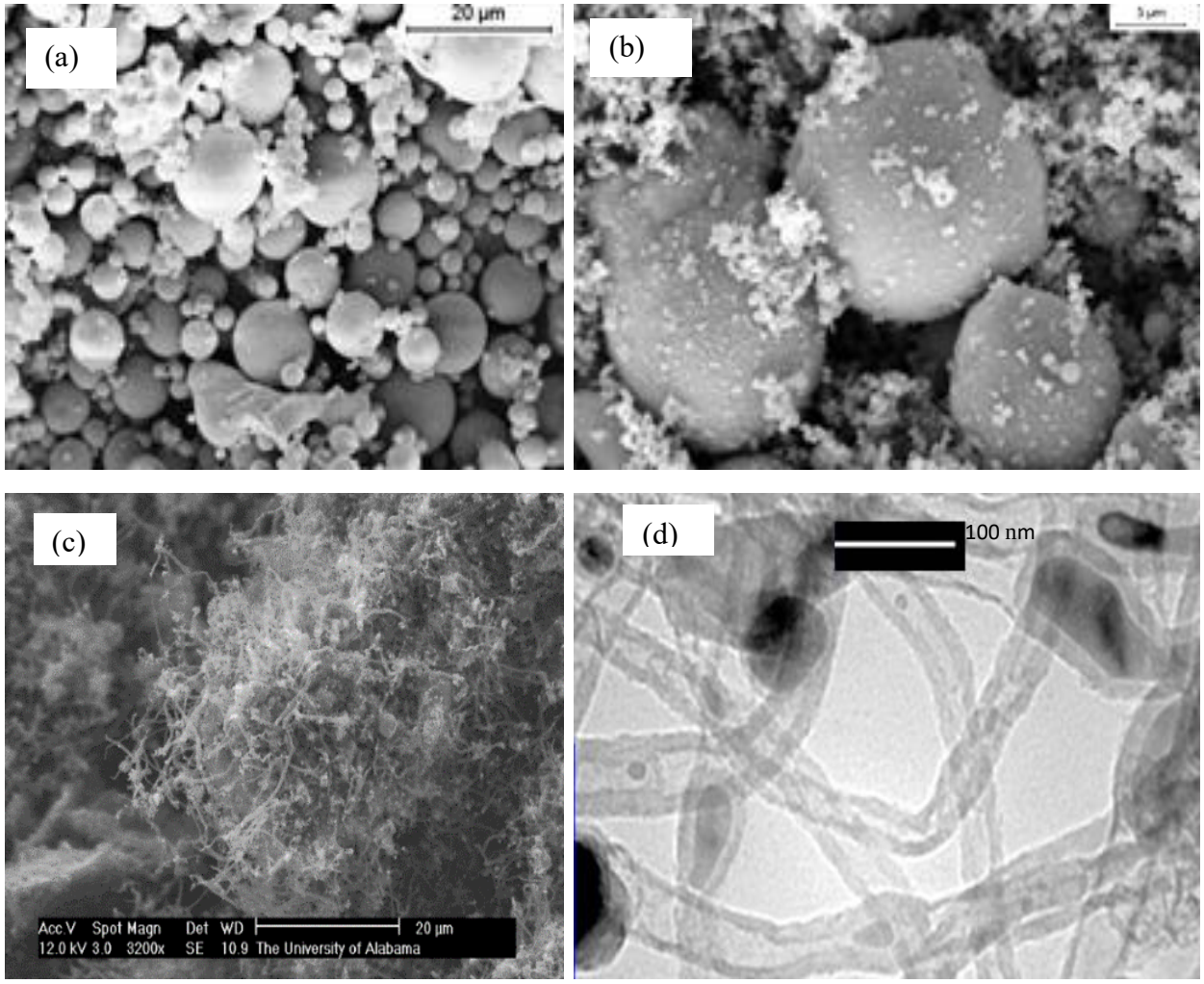

Figure 7. Growing CNTs on fly ash particles: (a) fly ash; (b) fly ash coated with polypyrrole; (c) fly ash with CNTs (microwave B with ferrocene); (d) TEM image of some hollow nanocarbons produced by Poptube method.

2.3.2 Effect of growing CNTs on the dissolution degree of fly ash

Dissolution testing shows that the dissolution degree of the plain fly ash is 57.2%. After grown this CNTs, this value was reduced drastically to 24.0%. This may suggest that

growing CNTs on the surface of fly ash can significantly reduce the reactivity of the fly ash. However, our previous study [15] shows that dissolution testing could be misleading because some reaction products can precipitate on the surface of the fly ash, and therefore, leading to lower measured dissolution degree than the real value. This can be seen in the conductivity testing and SEM images described as follows.

2.3.3 Effect of growing CNTs on the conductivity of fly ash suspension

Conductivity testing results at ambient temperature (23℃) are shown in Figure 8(a) shows the conductivity of the fly ash suspension before and after grown with CNTs in deionized water. The electrical conductivity of the plain fly ash suspension increases with time quickly after mixing with water. This is because the presence of soluble salts in the fly ash particles. These salts, especially those deposited on the surface of the fly ash, can be quickly dissolved in water and therefore, increase the concentration of ions in water. As a result, the electrical conductivity of the fly ash suspension increases with the testing time. After about 1 *h*, most soluble salts were dissolved in water and the conductivity of the suspension becomes stable, as shown in Figure 8(a).

Similar trend can be observed for the water suspension of the fly ash grown with CNTs. However, the conductivity of this suspension is much lower than that of the plain fly ash suspension. This can be attributed to less soluble salts available on the surface of the fly ash after growing CNTs on its surface. These salts could be either covered by the CNTs and the residue of the CNT precursor, or removed during the manufacturing process of CNTs using the Poptube method.

Figure 8(b) shows the conductivity of the fly ash suspension in 0.05M NaOH solution. After subtraction the contribution of the soluble salts to the conductivity shown in Figure 8(a), the

electric conductivity of this suspension changing with time due to the reaction between the fly ash and NaOH is shown in Figure 8(c), which exhibits three different stages. At the beginning of the testing, the conductivity of the suspension reduces quickly with time as soon as the fly ash is mixed with the alkaline solution. In this stage, the major reaction is the reaction between the soluble salt in the fly ash and NaOH, leading to fast reduction of the conductivity. This stage lasts about 30 mins. In the second stage, the conductivity varies very little with time, as shown in Figure 8(c). This suggests that no reaction between the fly ash and the alkaline occurred in this period. This is the induction period of the geopolymerization which lasts until 164 mins. At the end of this stage, the conductivity of the suspension increases sharply with time, indicating a fast dissolution period of the fly ash due to the attack of the alkaline solution. After this, the suspension enters the last stage, in which the conductivity of the suspension reduces with time, resulted from the chemical reaction between the fly ash and the alkaline solution.

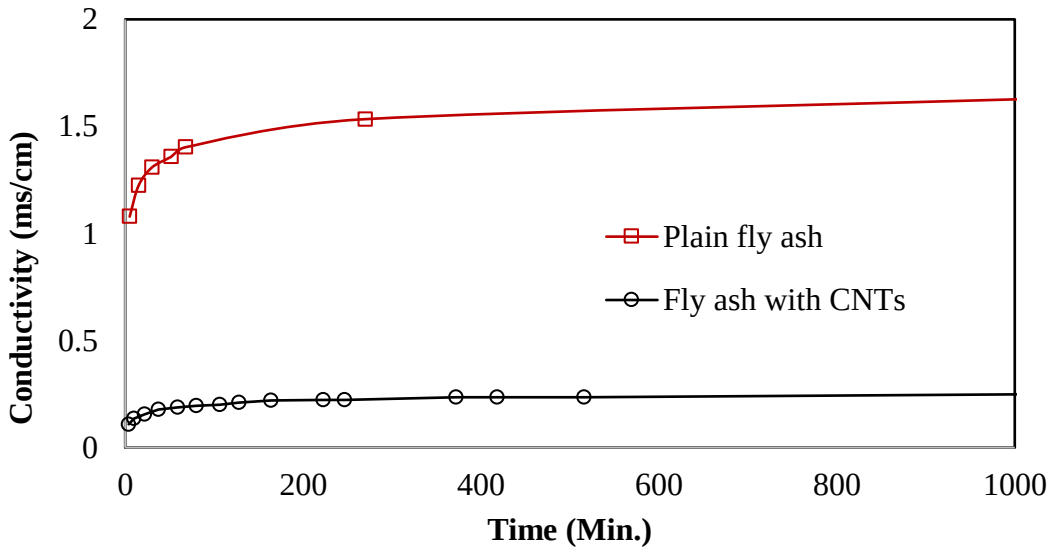

(a)

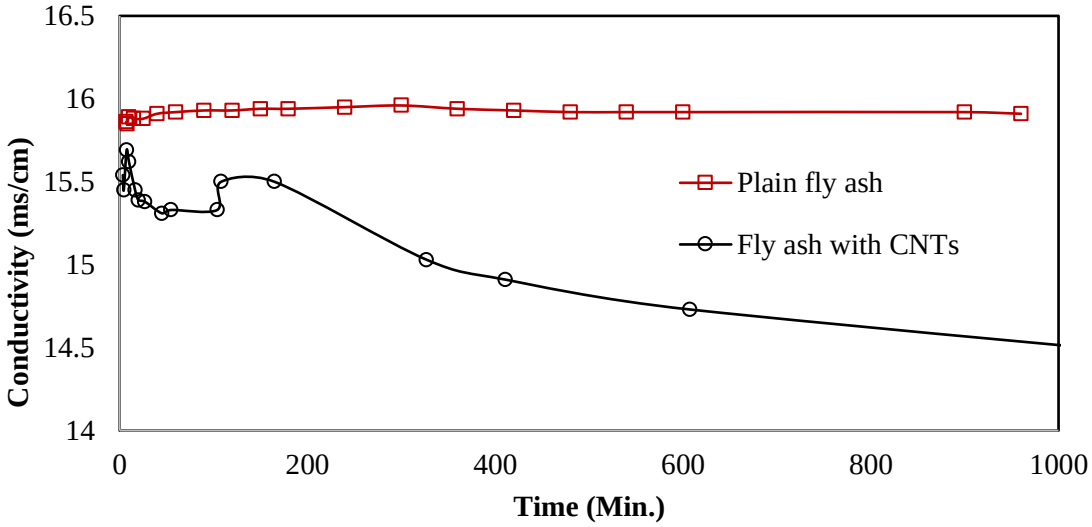

(b)

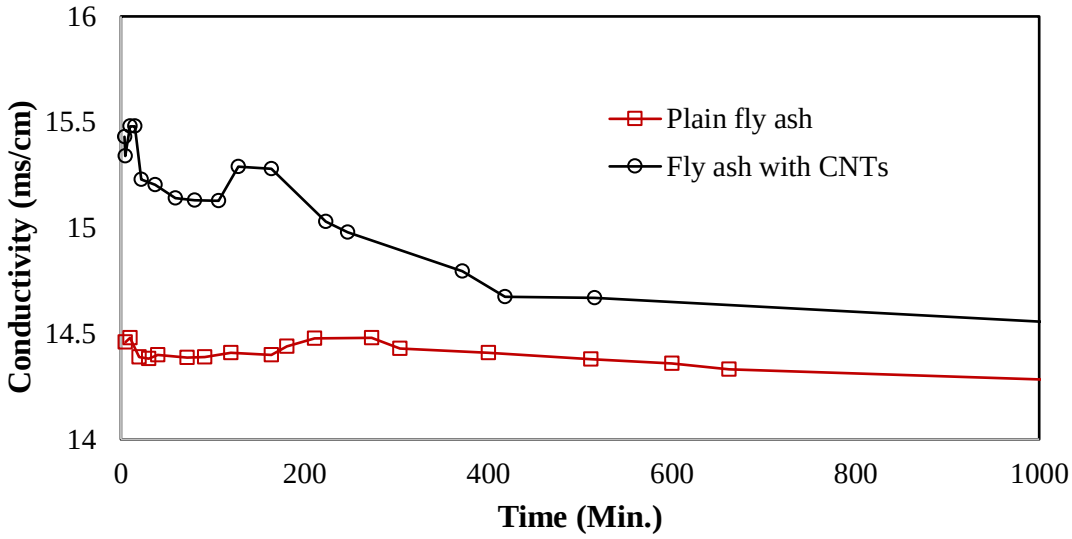

(c)

Figure 8. Conductivity of the fly ash in water and the alkaline solution at 23°C: (a) in purified water; (b) in 0.05M NaOH solution; (c) difference between (a) and (b)

Similar three stages can be also identified from the conductivity curve of the fly ash grown with CNTs in the NaOH solution, as shown in Figure 8(c). Overall, the conductivity of this suspension is higher than that of the plain fly ash. This is anticipated since the CNTs are highly electrically conductive. After mixing with the NaOH solution, some of the CNTs were pulled

away from the fly ash and dispersed in the suspension, making the conductivity of the suspension higher. It can be seen clearly that the second stage for this CNTs coated fly ash suspension in 0.05*M* NaOH solution is much shorter (about 84 mins.) than that of the plain fly ash suspension (140 mins.). This is because the CNTs on fly ash particles function as nucleation sites for the reaction between the fly ash and the alkaline activator, and therefore, reduce the induction time. This observation can be further confirmed by the length of the last stage. For the fly ash with CNTs, this third stage lasts about 310 mins., much shorter than 500 mins., the duration of the last stage of the plain fly ash suspension. Clearly, with CNTs, the reaction between the fly ash and the alkaline solution is much faster. This suggests that the CNTs grown on the surface of the fly ash can accelerate the geopolymerization process, which may compensate the reduced dissolution of the fly ash induced by the CNTs coverage. Indeed, the total reduction of the electrical conductivity of the suspension of the fly ash grown with CNTs is higher than that of the one with plain fly ash, indicating more reaction occurred in the suspension of the fly ash with CNTs.

Figure 9 compares the electric conductivity of the plain fly ash and fly ash grown with CNTs suspensions at 40°C. At this temperature, little difference can be found on the trend of the conductivity of the suspension varying with time from that at the ambient temperature. However, significant difference from that at ambient temperature appears on Figure 9(c). In this figure, three distinct stages present at ambient temperature becomes negligible in plain fly ash suspension. This is because the dissolution and reaction rates are accelerated at higher temperature. As a result, the dormant period is substantially reduced to negligible, if not fully eliminated. Similarly, the dormant period in CNTs coated fly ash suspension is also reduced to a slightly lower extent, as still can be observed from Figure 9(c). Compared with plain fly ash

suspension, the CNTs coated fly ash suspension exhibits much higher reduction on electric conductivity, suggesting more reaction is induced by growing CNTs on the surface of the fly ash. This agrees with the observation at ambient temperature. Compared with Figure 8(c), Figure 9(c) shows that total reduction of the electric conductivities for both suspensions are higher than their counterparts at ambient temperature, suggesting that more reaction is accomplished at 40℃

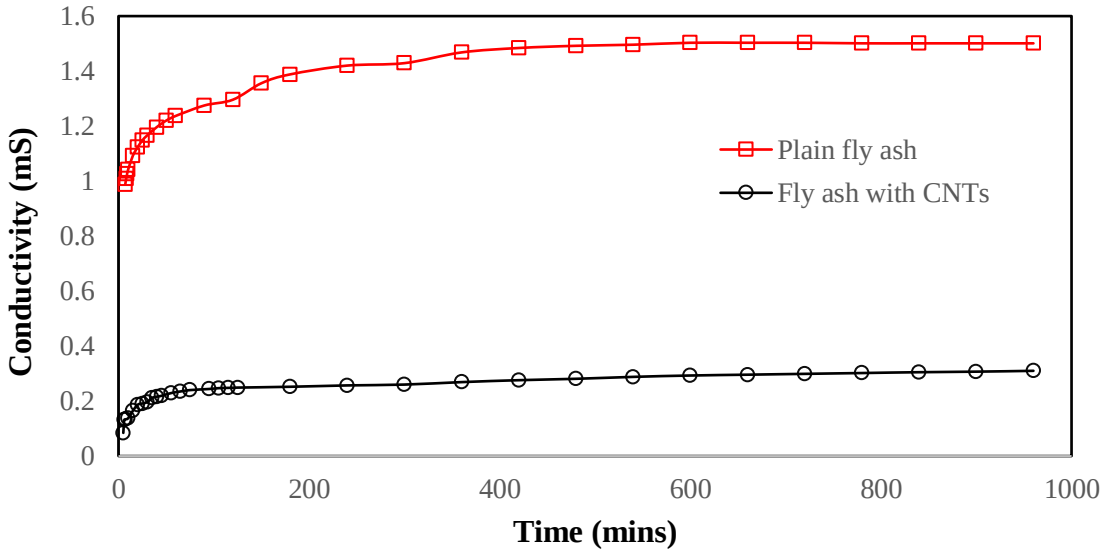

(a)

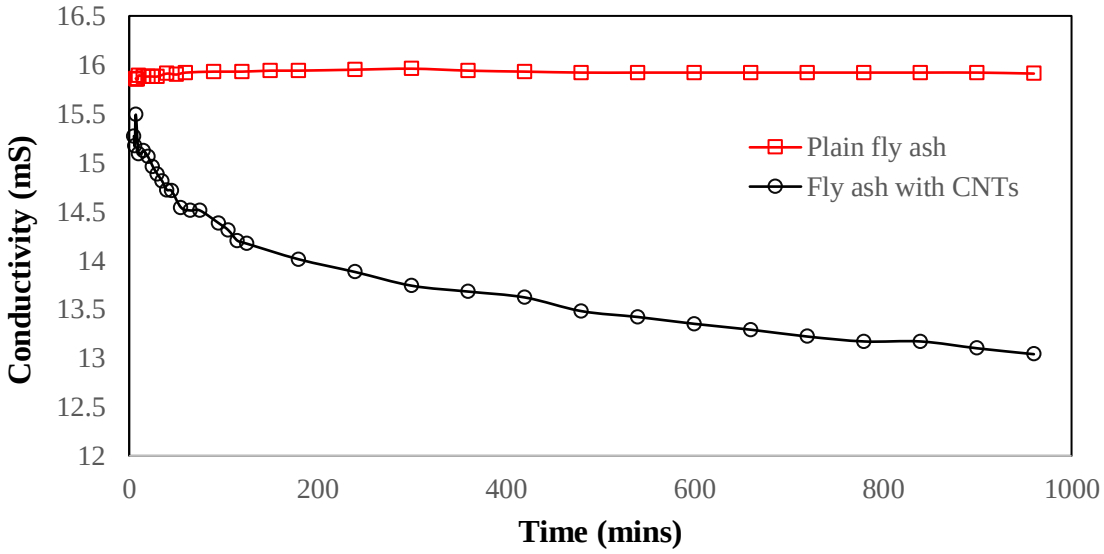

(b)

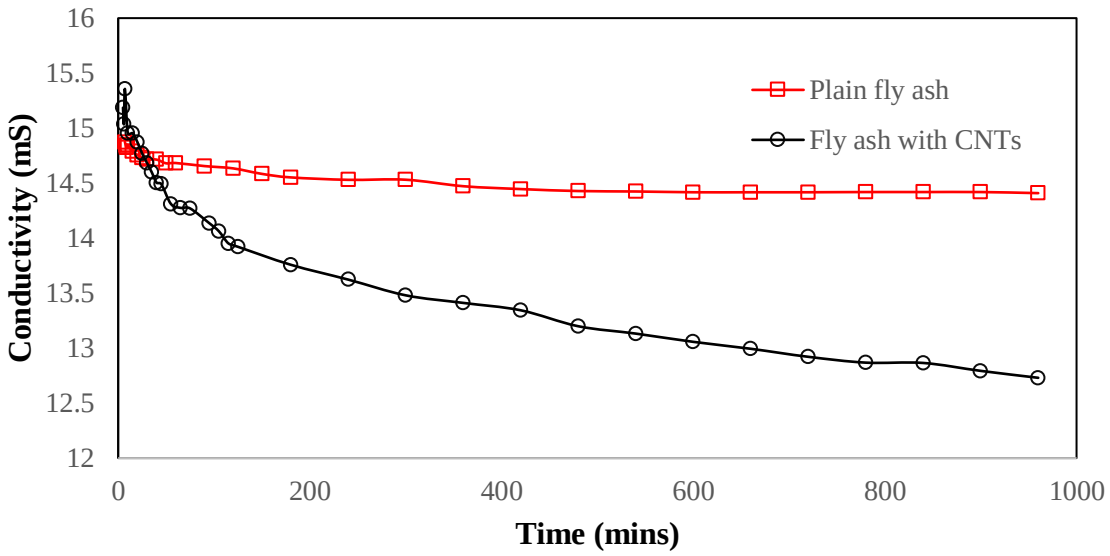

(c)

Figure 9. Conductivity of the fly ash in water and the alkaline solution at 40°C: (a) in purified water; (b) in 0.05M NaOH solution; (c) difference between (a) and (b)

2.3.4 SEM examination of fly ash in alkaline solution

The above observation can be further confirmed by the SEM images of a single fly ash particle exposed to the NaOH solution, as shown in Figure 10(a) shows a fly ash particle embedded within the epoxy before exposed to the NaOH solution. It can be seen that half of the fly ash particle was removed by grinding and polishing. A small piece of residue can be found on the upper left corner of this fly ash particle. After 24*h* exposure to the alkaline solution, reaction products between the fly ash and the NaOH solution can be found mainly deposited on this piece of residual material, as shown in Figure 10(b). Figure 10(c) shows a fly ash particle grown with CNTs after exposure to the NaOH solution. Most of its surface is covered by new precipitate, which was induced by the seeding effect of the CNTs. The difference observed in Figure 10(b) and Figure 10(c) provides a possible reason for the low dissolution degree measured for the fly ash grown with CNTs. The CNTs on the surface of the fly ash particle can retain some dissolved

chemicals from the fly ash or reaction products between the fly ash and NaOH. As a result, the measured dissolution degree which is based on the loss of mass tends to be higher than its real value.

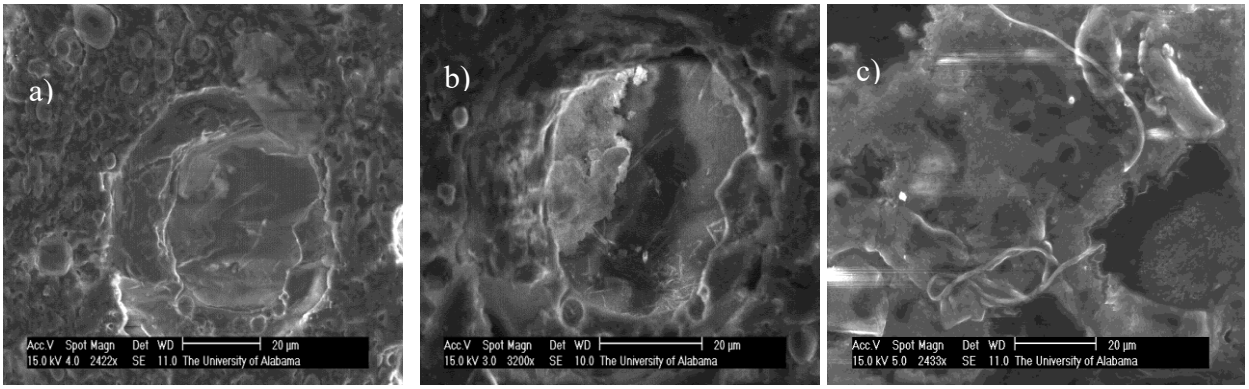

Figure 10. SEM images of a single fly ash particle exposure to NaOH solution: (a) plain fly ash particle before exposure; (b) plain fly ash particle after 24 hours exposure; (c) fly ash particle grown with CNTs after 24 hours exposure.

2.3.5 In-situ observation of fly ash dissolution in alkaline solution using AFM

Figure 11 shows the surface topography change of a fly ash particle in alkaline solution at 0h, 2h, and 4h obtained by AFM. Figure 11(a) shows that some small powders were attached to the fly ash particle at 0h, which are very likely some soluble salts. After 2h in alkaline solution, these powders disappeared as shown in Figure 11(b), suggesting that they were dissolved into the alkaline solution. It is interesting to see that many grooves are present on the surface of the fly ash after 4h in alkaline solution (Figure 11(c)). These grooves should be created by the dissolution of fly ash in the alkaline solution. This indicates that the dissolution of fly ash is not uniform on the surface of the fly ash. Rather, it starts with some active sites, which will propagate and grow into "grooves" as revealed by the AFM topography images shown in Figure 11.

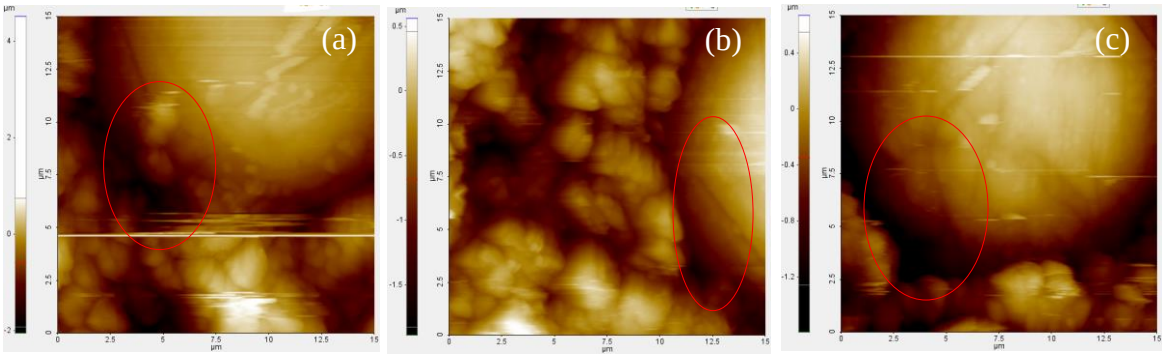

Figure 11. Fly ash particle in alkaline solution under AFM (a) 0h; (b) 2h; (c) 4h

2.3.6 In-situ observation of geopolymerization using AFM

SEM images are produced in a vacuumed environment with no allowance of presence of liquid; therefore, it is difficult to use SEM to monitor any changes in the early stages of geopolymerizaiton. This disadvantage of SEM can be eliminated by using an AFM. The AFM has the ability to form images in ambient environment. This function, along with the non-contact electrostatic force mode, makes the nanometer- scale in-situ geopolymerization monitoring possible. The in-situ monitoring simulates the process of lab geopolymer sample making more accurately than the previous method. Therefore, the result could provide a more accurate reference for future productions of geopolymer.

A circular aluminum deck of diameter D = 1.0 cm and thickness T = 0.1 cm was glued with a #6 copper flat washer to provide a platform for the purpose of the in-situ conductivity testing of the Gaston fly ash geopolymer. Such platform was later be placed into the AFM chamber as the conductive deck and the holder of the freshly mixed geopolymer fluid. The freshly mixed geopolymer was made with mix as fly ash : water : sodium hydroxide : sodium silicate = 62 : 8.5

: 7.5 : 22. To model the process of geopolymerization, it is essential to keep the moisture content of such small volume of the freshly mixed geopolymer. Therefore, the platform was sealed by clear plastic films, only leaving a small opening on top for the AFM analysis, after the fluid was placed into the platform.

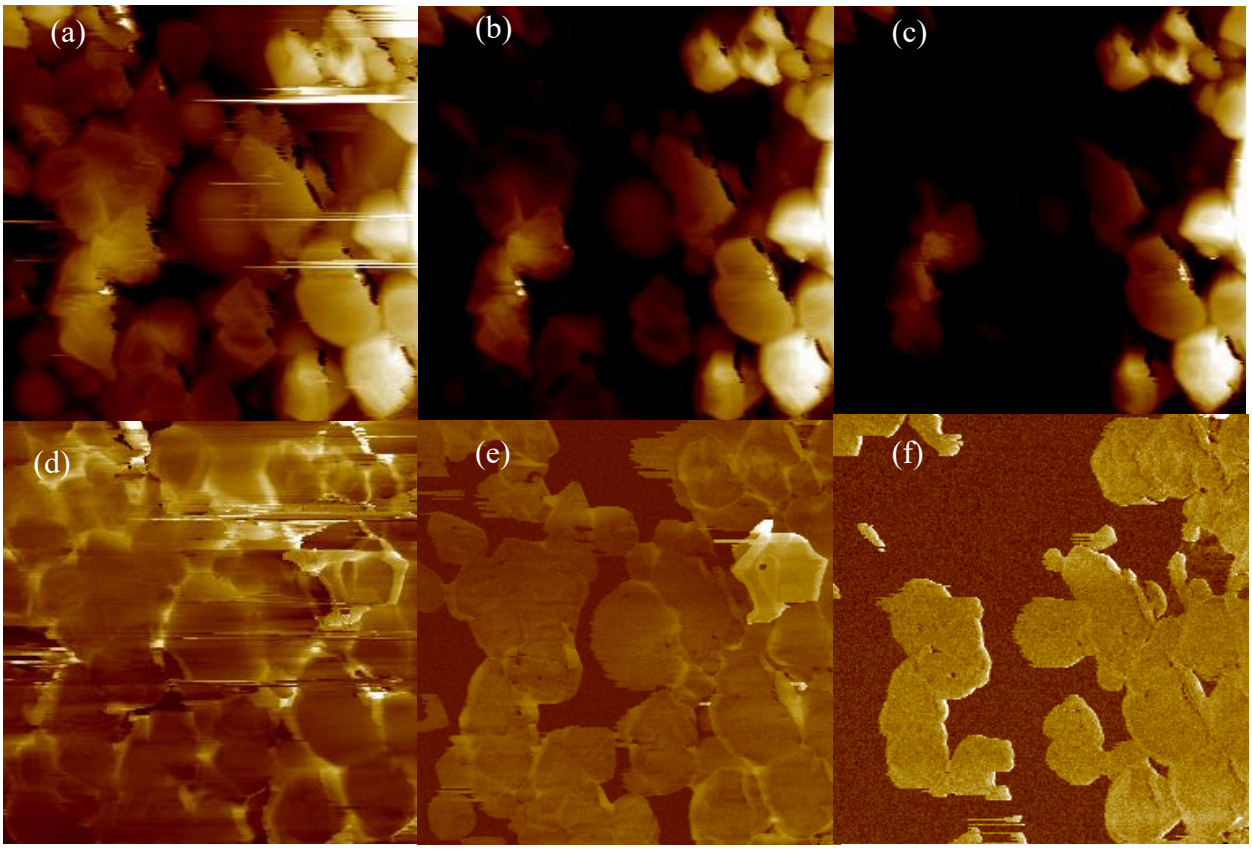

Figure 12. AFM topography and current images for different time after mixing: top row: topography images, (a) 60mins; (b) 120 mins; (c) 180 mins; bottom row: current images, (d) 60mins; (e) 120 mins; (f) 180 mins

AFM imaging results are shown in Figure 12. Figure 12(a-c) show the topography image of the geopolymer sample at 60 min, 120 min, and 180 min. At 60 min, a spherical fly ash particle can be observed, surrounded by hydration products. One hour later, the topography image becomes darker, suggesting that the surface height of the observed area is reduced. This can be attributed to the evaporation of moisture, which can lead to significant shrinkage in geopolymer.

This shrinkage increases with reaction time, as shown in Figure 12(c). After 180 min reaction, the surface height in the observed area became even lower, which makes it difficult to observe the geopolymerization process. Therefore, current images were obtained and shown in Figure 12(d-f).

The electric current is a measurement of local charge in the geopolymer. At first 60 min, the electric charge in the geopolymer sample is very high, as shown in Figure 12(d). It can be seen that the charge in the solution between solid particles is extreme high, as indicated by the very bright color in these zones. This suggests that at this early age, the activation solution is very rich in many ions and major precipitation to form geopolymer may not start yet. After one-hour reaction (Figure 12(e), the color of the pore solution between solid particles were much darker, suggesting that charged ions in the pore solution were largely consumed by the geopolymerization. A light-color edge can be found for most solid particles, suggesting that geopolymerization process is undergoing at these zones. One hour later, the bright color in the pore solution completely disappeared, indicating further development of the geopolymerization (Figure 12(f)). Figure 12(f) also shows that some solid particles cannot be observed, suggesting that they were covered by the geopolymer precipitate. This precipitate has relatively low charge, and therefore, cannot be distinguished by the AFM from its surrounding pore solution. In addition, only a small portion of the edge of the solid particle has a bright color, indicating most geopolymerization process has been accomplished at this time.

2.4 Conclusions

In this chapter, the reactivity of fly ash before and after growing CNTs has been examined by a few experimental studies. Some conclusions can be drawn based on these testing results.

1) Conductivity testing revealed that reaction between the fly ash and NaOH can be divided into three stages: the fast dissolution stage at the beginning in which the conductivity of the suspension reduces quickly with time due to the reaction between the soluble salt in the fly ash and NaOH; the dormant stage in which the conductivity varies very little with time as reaction between the fly ash and the alkaline has yet started, and the geoploymerization stage in which the conductivity of the suspension increases sharply with time, and then reduce with time, resulted from the chemical reaction between the fly ash and the alkaline solution.
2) Growing CNTs on the surface of fly ash doesn't reduce the reactivity of the fly ash. Instead, the CNTs on the fly ash can function as nucleating sites, which can accelerate the dissolution and precipitation of reaction products of fly ash in alkaline solution, as revealed by conductivity testing and SEM study.
3) AFM provides a good tool to in-situ observe the dissolution of fly ash and early-age geopolymerization process. It shows that dissolution of the fly ash in alkaline solution is not uniform in the surface of the fly ash particle. It appears that dissolution has favorable sites and grows in favorable directions. As a result, many grooves on the surface of fly ash can be observed, which are generated by the dissolution of fly ash in these locations.
4) AFM can be used to in-situ examine the early-age geopolymerization process. The topography image shows that drying shrinkage is significant in geopolymer, even at very early age. While the electric current measurement can provide a mapping of ion charges

on the surface of the geopolymer. Testing results show that ion charges which is very high in the aqueous phase of early age geopolymer was consumed after geopolymerization started. Once reaction products covered the surface of solid particles in the early age geopolymer, the charge on the surface of these particles were substantially reduced.

3. SYNTHESIS AND CHARACTERIZATION OF SELF-DISPERSING, SELF-SENSING GEOPOLYMERIC NANOCOMPOSITE USING POPTUBE METHOD

3.1 Introduction

Although extensive studies have convincingly shown that geopolymers possess much better strength and durability properties than OPC, they are brittle in nature and relatively weak under tension thus limiting their applications in many areas. The objective of this study is to strengthen the geopolymer with CNTs to overcome this weakness of geopolymers. The excellent electric conductivity of CNTs will add self-sensing ability to the produced geopolymeric nanocomposite.

Fly ash grown with CNTs using Poptube method is used to synthesize the nanomaterials. As illustrated in Figure 13. The fly ash particles grown with CNTs are first uniformly blended with the rest fly ash particles without CNTs. The resulted blended source materials are then mixed with alkaline activator. Once fly ash particles contact alkaline solution, hydrolysis reaction is initiated. With the aluminate and silicate species dissolve from fly ash particles into the solution, CNTs will be liberated and dispersed homogeneously nearby the fly ash particles. In this way, CNTs are self-dispersed in the material. After geopolymization is finished, these CNTs form a network, which will add self-sensing ability to the produced nanomaterial. The common approaches of dispersing CNTs, including sonication and chemical fictionalization, are avoided. This self-dispersing method makes it possible to manufacture large volume of geopolymeric nanocomposite quickly and continuously.

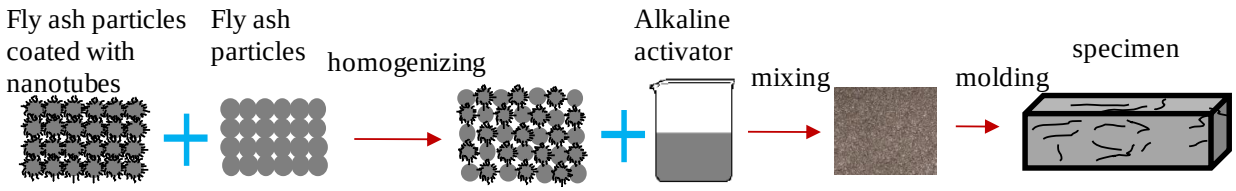

Figure 13. Illustration of synthesis process of self-dispersed geopolymeric nanocomposite

3.2 Materials and Methods

3.2.1 Materials

Same plain fly ash studied in previous chapter and the fly ash grown with CNTs produced in previous chapter were used to synthesize CNTs reinforced geopolymeric nanomaterials. Lab level sodium hydroxide and sodium silicate solution were obtained from Fisher Scientific. Sodium silicate solution contains 29.4 wt. % of SiO_2, 9.1 wt. % of Na_2O, and 61.5 wt. % of water.

3.2.2 Manufacturing of mortar samples using the geopolymeric nanocomposite as the binder

Two groups of mortar using geopolymer binder were made. One control group was made with the plain fly ash-based geopolymer. The self-sensing group was made by using the geopolymeric nanocomposite as the binder. A mix of NaOH solution and sodium silicate solution was chosen as the activator of the geopolymer. The mix design of the control group is chosen as sand : fly ash : sodium silicate : NaOH solution = 60 : 24.5 : 8.7 : 6.8. The self-sensing group was made by replacing 50% of plain fly ash with CNT-grown fly ash. Superplasticizer was added as 2.0% weight of the fly ash to enhance the workability. After cast into molds, mortar samples were first stored in the laboratory for two hours before they were put into the oven for curing for 24 *h* at 75°C. Cylindrical samples of mortar with size of 50 mm × 100 mm were manufactured to measure the compressive strength in compliance with ASTM

C39-05. Before testing, specimens were capped with sulfate cement so that both surfaces were flat and parallel. The compressive strength and modulus of the mortars were measured as the average of three duplicated specimen.

3.2.3 Measuring stress transfer between the geopolymer matrix and the CNTs using Raman Spectrometer

To reach the full potential of CNT reinforcement, stress must be effectively transferred from the matrix to the CNTs. However, to measure this stress transfer is one of the most difficult problems in the physics of nanocomposites [102]. In this study, a novel method using Raman spectrometer was developed to measure this stress transfer in the geopolymeric nanocomposite.

Raman spectra have been used to study stress transfer in fiber reinforced composites for over two decades. The Raman peaks of some fibers, such as carbon, Kevlar 49, shift to lower frequency when the fiber is under tension [103]. Similar phenomenon has also been observed in CNTs composite [104, 105]. The D-band of CNTs shifts with applied stress. However, this shift of D-band is not consistent or significant when CNT nanocomposite specimen is subjected to uniaxial force [104, 105] because of the random distribution of CNTs in the composite. If a CNTs in the nanocomposite is along the same direction of the tensile force, it is under tension. If perpendicular to the tensile force direction, the CNT is under compression due to Poisson's contraction. Therefore, the measured Raman signals are actually the average of all CNTs in all directions within the laser spot of the Raman Laser [106]. This averaging makes accurate measuring stress in CNT impossible. To overcome this difficulty, hydrostatic stress should be applied so that all CNTs in the nanocomposite are under the same stress. Lourie and Wager [107] implemented this idea by measuring the nanocomposite at different temperatures. The difference in coefficients of thermal expansion between the CNTs and the matrix introduce a thermal stress

within the composites, which are uniform in any direction. As a result, very significant D-band shift was observed in their study [107].

Lourie and Wager's approach was adopted in this study. A Raman spectroscope with 633 nm excitation (with Olympus IX71 inverted microscope) was used for the experiment, as shown in Figure 14(a). A thin geopolymeric nanocomposite was placed on an Indium tin oxide (ITO) platform, as shown in Figure 14(b). ITO is electrically conductive so it can be heated by applying an electric potential. It is also transparent, so it doesn't interfere with the measurement of Raman spectra. The ITO piece was calibrated to establish the relationship between the applied electric potential and the temperature at the center of the ITO cover slip (22x22 mm 15-30 Ω spi® supplies). During the calibration, the applied voltage was increased at a 1.00 V interval. The temperature was recorded every minute for 10 minutes after each increase in voltage. The calibration started from 5V to 20V. In this way, the temperature of the nanocomposite sample can be controlled by the applied voltage. One-second-per-frame readings were used to help allocate a good location which represents the peaks of the Rama spectrum the best. After that, 6 ten-second-per-frame readings were used for each applied voltage. Each Rama spectrum reading started roughly 3 minutes after each increase in voltage to ensure a stabilized and uniform temperature over the specimen. Eight groups of readings were obtained starting from room temperature (25°C) to 109°C. The difference in the coefficients of thermal expansion between the CNTs and the geopolymer matrix introduces a thermal stress within the nanocomposite, which are uniform in any direction. The stress in the CNTs can be measured by the shift of the D-band of the Raman spectrum of CNTs.

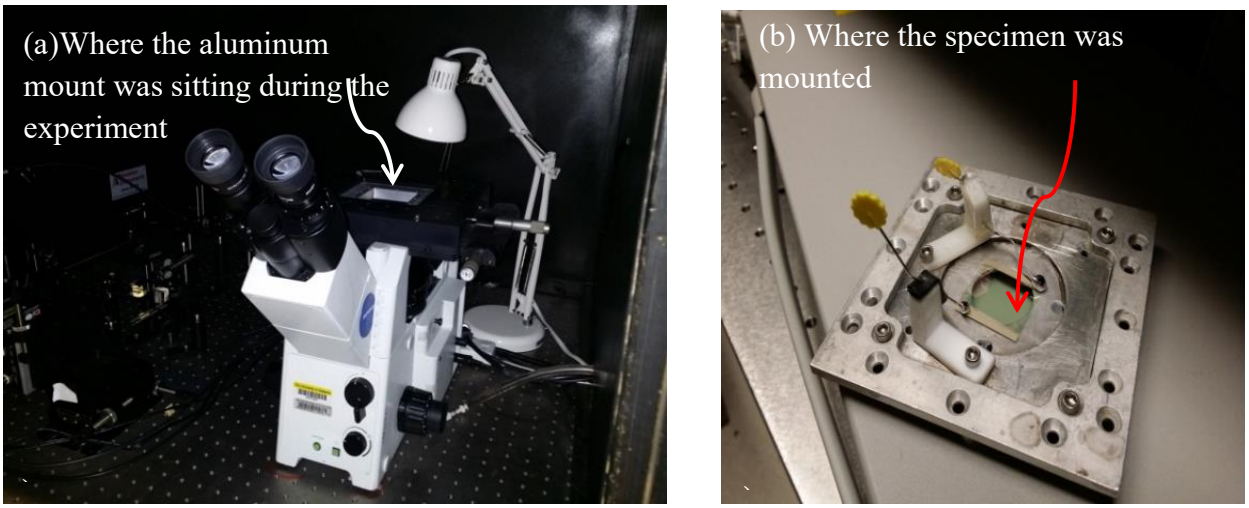

Figure 14. Testing set-up to measure stress transfer in the geopolymeric nanocomposite: (a) testing set-up; (b) ITO platform used to mount and heat the nanocomposite sample

3.2.4 Evaluating the self-sensing function of the mortar

A four-electrode-DC method, which was commonly used by existing studies, is employed to evaluate the self-sensing function of the mortar samples, specimens with 20 mm x 20 mm x 50 mm were made with four electrodes with 20 mm (inside pair) and 40 mm (outside pair) apart from each other (Figure 15(a)). A 5V DC current generated by an Agilent 33220A wave generator was applied to two electrodes, and an Agilent 34410A 6 1/2 digit multi-meter was used to measure the electric current from another two electrodes. The whole specimen was subjected to compressive load applied through an MTS QTEST/25 machine. The whole testing set-up is shown in Figure 15(b). Then, periodic loading was applied to the specimen. In the meantime, the current of the specimen was measured by a multi-meter to determine the change of the resistivity of the specimen.

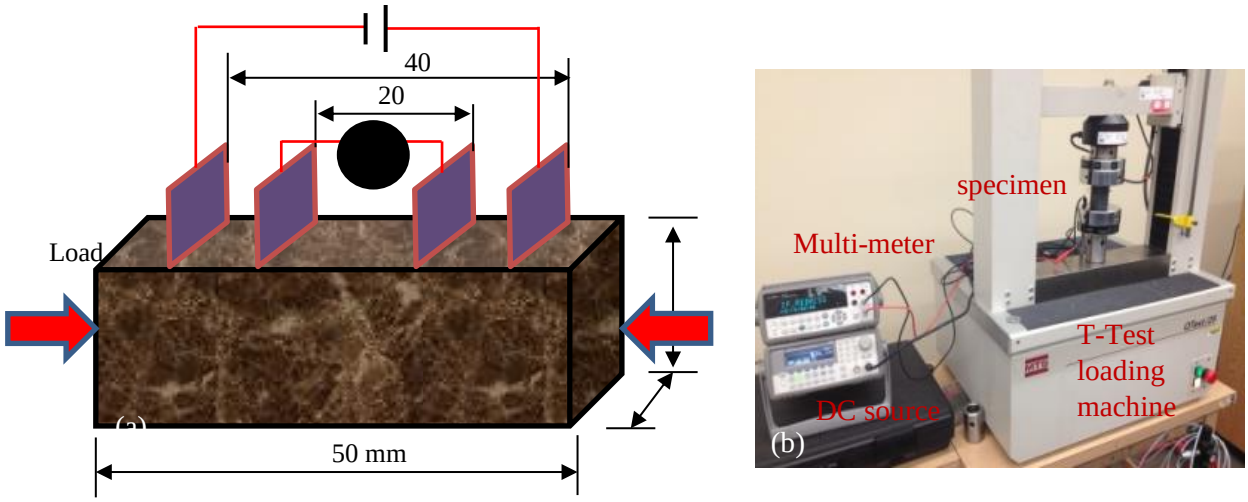

Figure 15. Self-sensing testing of the geopolymeric nanocomposite: (a) schematic of the specimen; (b) Testing Set-Up

3.3 Results and Discussion

3.3.1 Compressive strength and microstructure of mortar with goeopolymeric nanocomposite

The compressive strength of the mortar sample using plain geopolymer binder was measured as 64.7 MPa. The compressive strength of the mortar using geopolymeric nanocomposite binder was determined as 70.7 MPa, which is slightly higher (9%) than that of the control group. This enhancement of compressive strength induced by the CNTs reinforcement is rather moderate, mainly attributed to the poor microstructure of the nanocomposite adjacent to the fly ash particles grown with CNTs, as shown in Figure 16. This figure compares the microstructures of the plain geopolymer (Figure 16(a)) and the geopolymeric nanocomposite (Figure 16(b)). It can be seen clearly that although the CNTs on the fly ash surface can serve as nucleating sites for geopolymerization, the presence of these CNTs could affect the wettability of the fly ash particle, leading to rather porous structure near the fly ash particle (Figure 16(b)). This porous structure

can offset the reinforcing effect of the CNTs. As a result, the strength increase induced by the CNTs reinforcement is very limited.

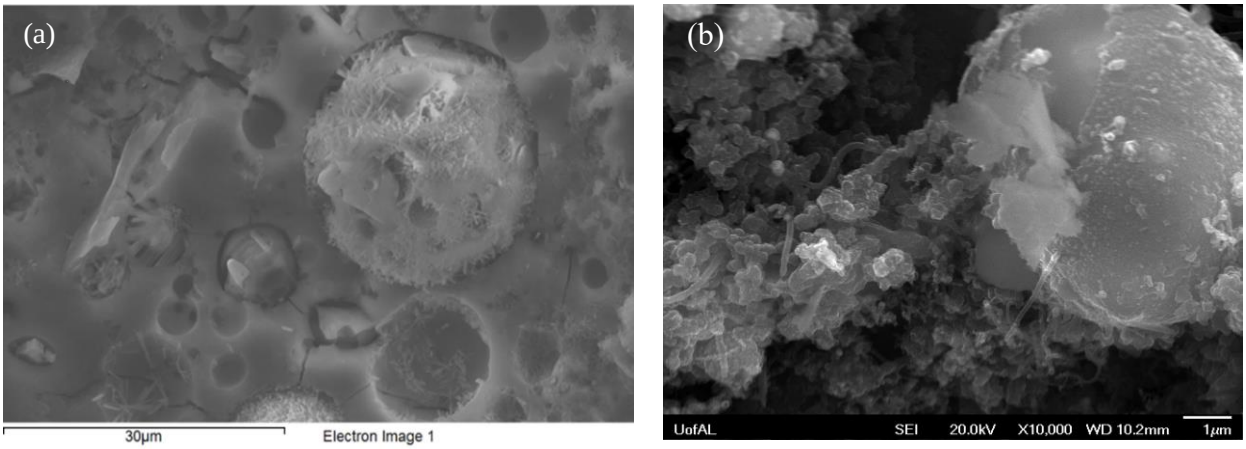

Figure 16. Microstructures of (a) geopolymer made with plain fly ash; (b) geopolymeric nanocomposite made with fly ash grown with CNTs

3.3.2 Stress transfer between the geopolymer matrix and the CNTs

Figure 17(a) shows the Raman spectra of the geopolymeric nanocomposite under different temperatures. The shift of D-band can be seen more clearly in the close-up given by Figure 17(b). Figure 18 shows that the D-band shifts to higher frequency with temperature and moves back with temperature drop. This shift of D-band with temperature clearly suggests that composite effect exists between the CNTs and the geopolymer matrix and that stress can be effectively transferred from the matrix to CNTs. Once temperature is reduced as shown in three cooling curves in Figure 17, the D-band reduces too, as shown in Figure 18. However, exact overlap with the heating path is not achieved in Figure 18. This is clearly due to the re-adjusted thermal stress with the nanocomposite. Figure 18 also shows that the shift of the D-band almost linearly increases with temperature, indicating that the proposed method can be used as a non-contact method to measure the stress in CNTs.

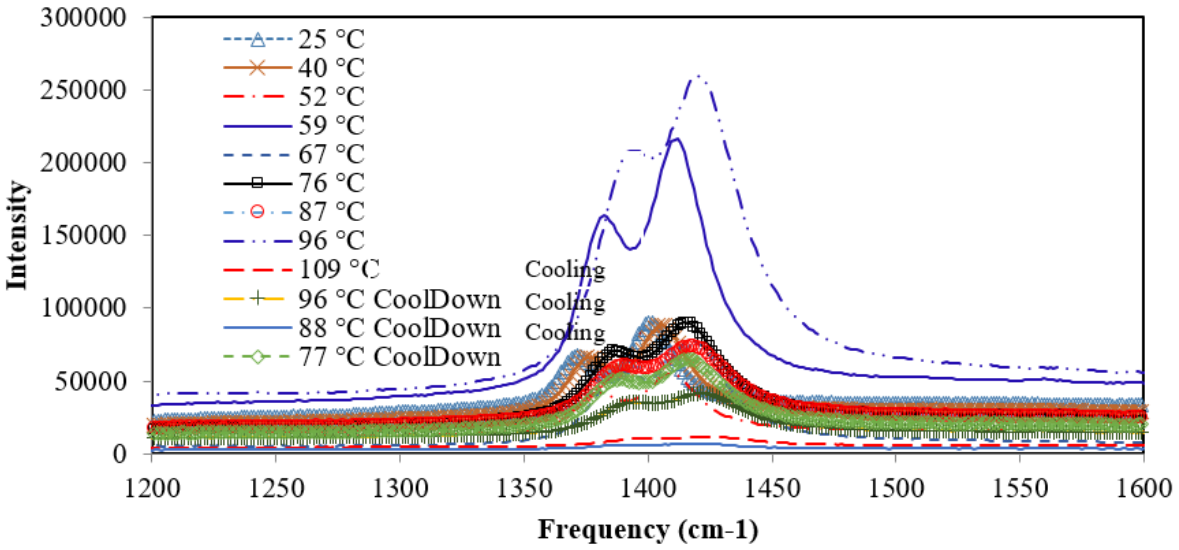

(a)

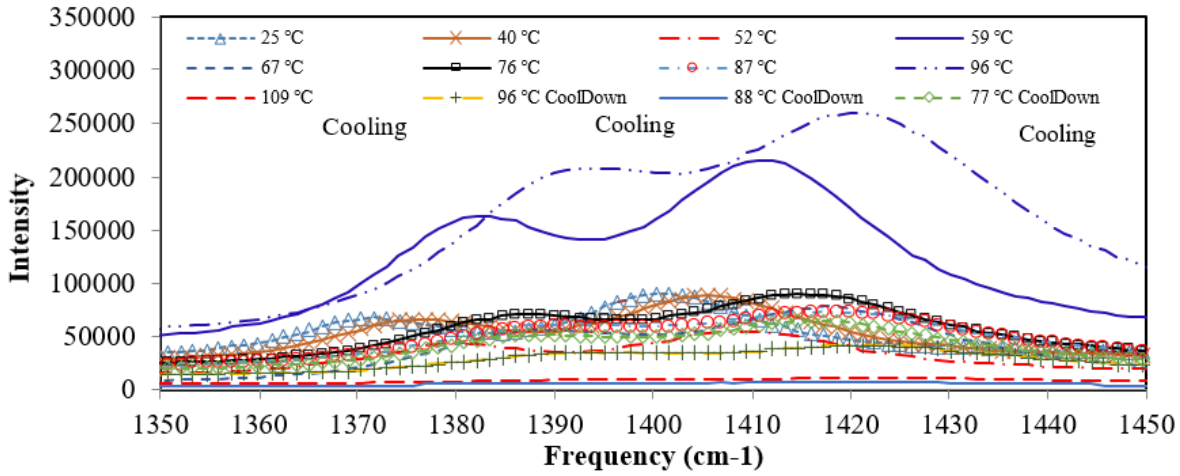

(b)

Figure 17. D-band shift of geopolymeric nanocomposite under thermal stress: (a) Raman spectra of the geopolymeric nanocomposite specimen under different thermal expansion; (b) Details of D-band shifts under different thermal expansions.

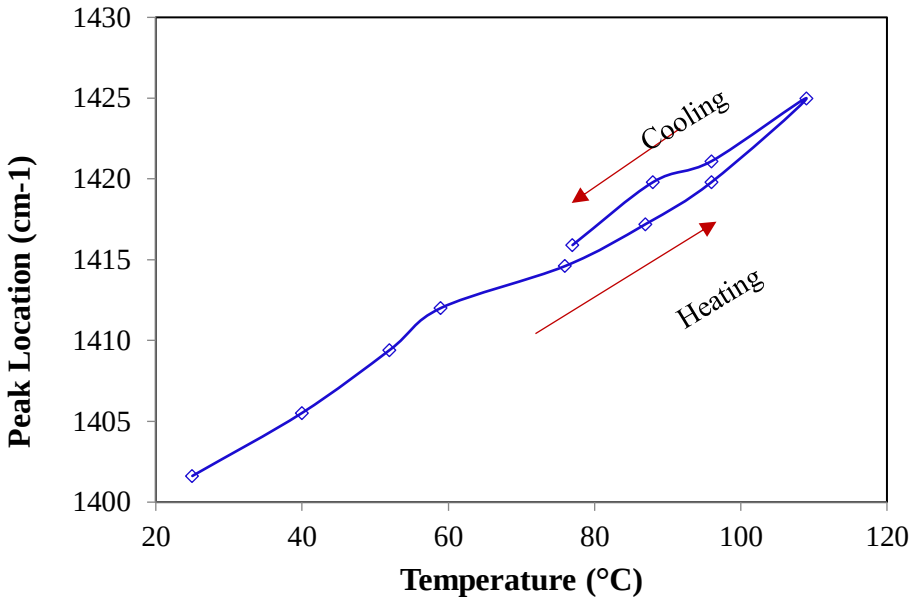

Figure 18. D-band shift of the geopolymeric nanocomposite with temperatures

3.3.3 Self-sensing function

Figure 19 shows the loading history and the corresponding resistance of the control geopolymer mortar sample at 4d after the specimens was cast. Interestingly, the electric resistance of the specimen varies in proportion to the applied load, indicating that mortar sample can sense the applied load even without CNTs. The piezoresistivity exhibited by the geopolymer itself is mainly caused by the ion's conductivity at the early age of the geopolymer. As revealed in electric conductivity study before [108], geopolymer has very high electric conductivity at its early age. Time drift can be clearly seen in the in the electrical resistance signals, as shown in Figure 19, which is caused by the polarization effect of the DC current used to measure the resistance of the sample, which is a common problem in many existing studies [109].

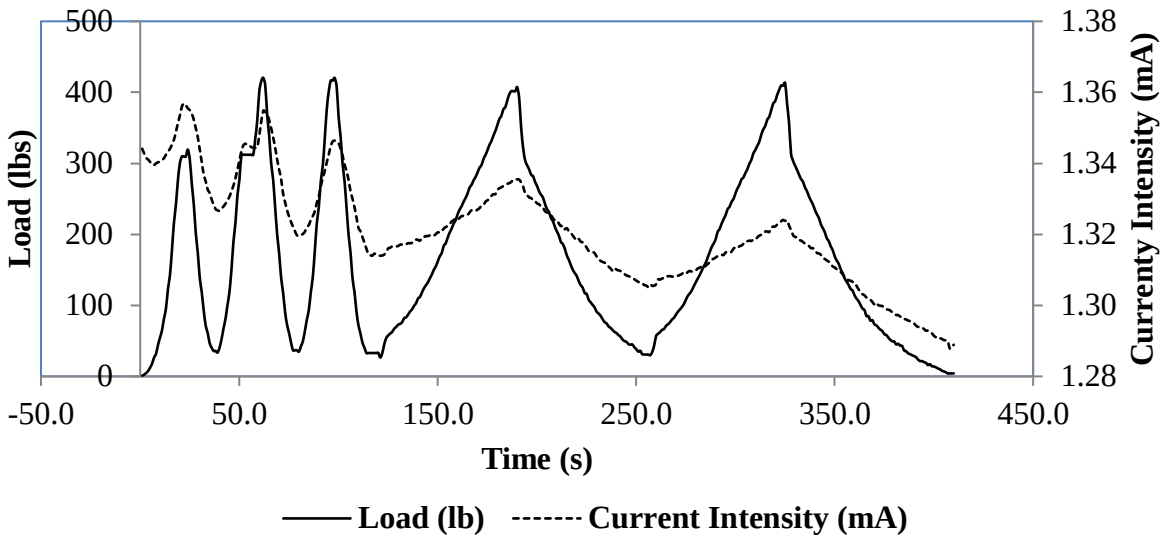

Figure 19. Periodic loading test 4 days after specimen was molded (control)

The next test was performed 15 days after the pouring. As shown in Figure 20, the current intensity was substantially reduced, indicating that available free ions were much less in the mortar after 15d reaction. Similar to the case of 5d, current intensity also reduces with the loading cycle, induced by the polarization effect of the DC current.

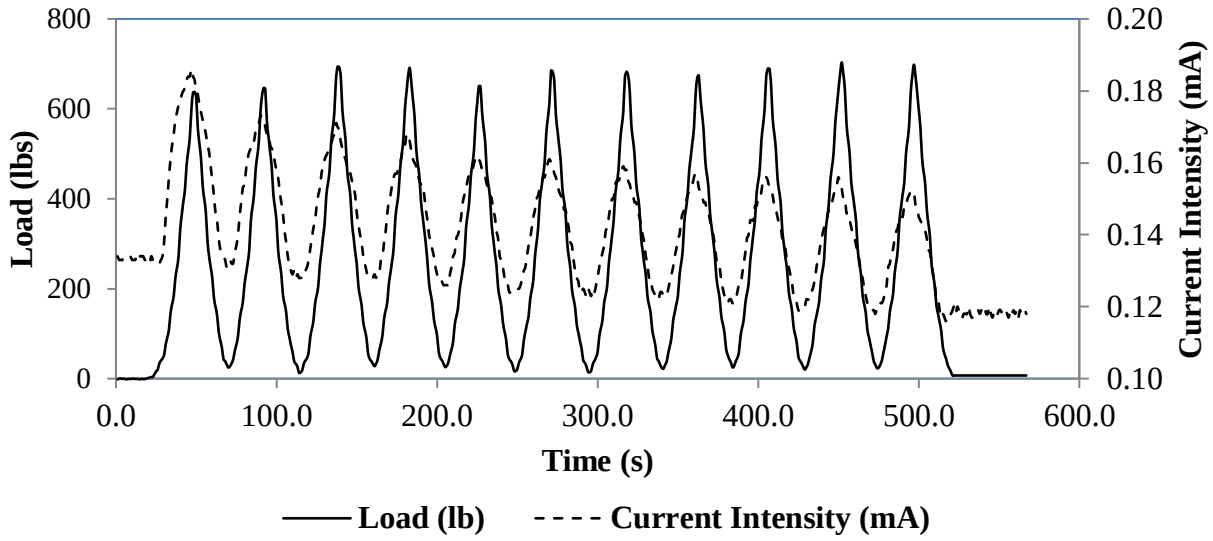

Figure 20. Periodic loading test 15 days after specimen molded (control)

Figure 21(a) shows the current intensity vs. applied load of the control specimen without CNTs at age 35d. Similar to the cases of earlier ages, the electric current varies in proportion to the applied load, confirming that the geopolymer mortar at this age is still piezoresistive. Although the stress applied is four time as the one used at 5d, the measured current is lower than that at 5d, suggesting that geopolymerization is more completed at 35d. This can also be confirmed by the almost negligible drift of the electric current. Clearly, at this age, free moving ions in the sample is very little, reducing the polarization effect of the DC current.

Figure 21(b) presets current intensity vs. applied load of the geopolymeric nanocomposite with CNTs at age 35d. As expected, the measured current is in proportion to the applied stress, confirming the self-sensing ability of this material. More importantly, the current intensity of this material is almost 2000 times higher than that from the geopolymer specimen (Figure 21(a)). Clearly, such a huge improvement on electric current intensity is caused by growing CNTs on fly ash particle, making it much more sensitive than the control one for stress sensing.

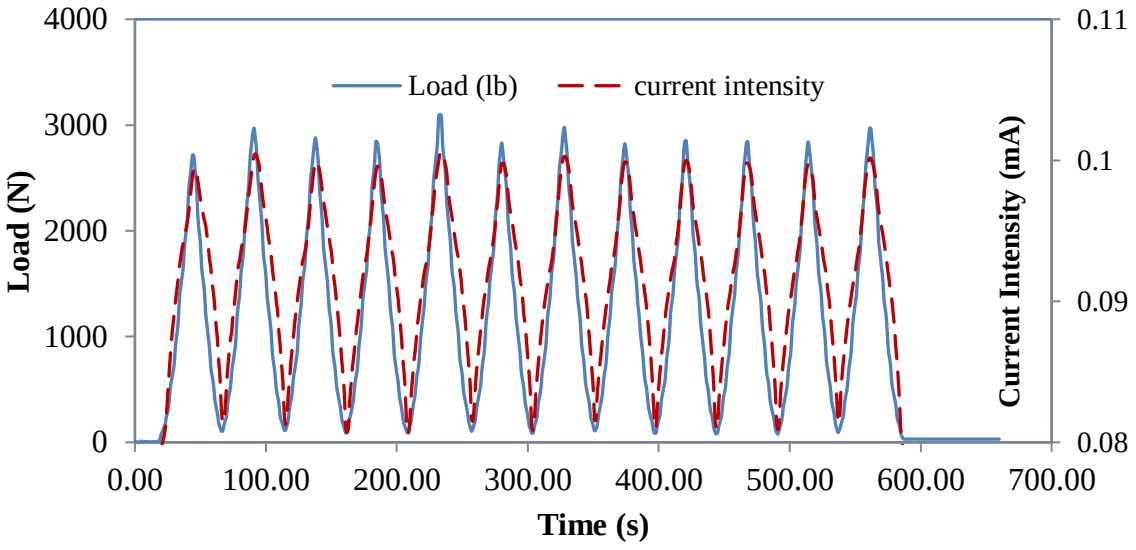

(a)

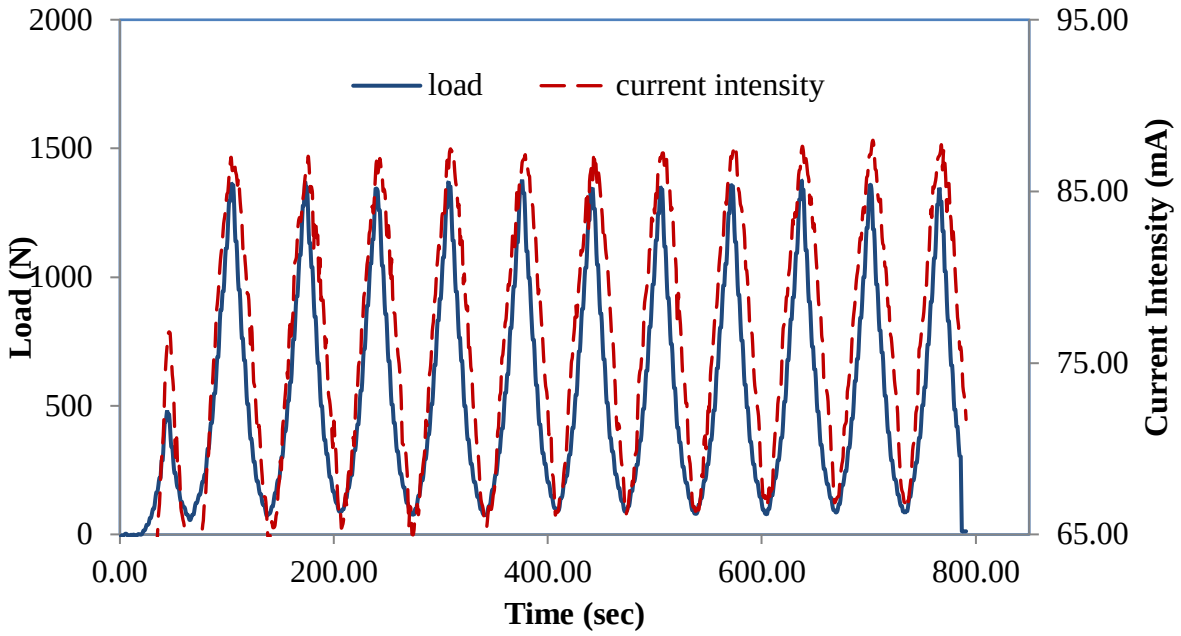

(b)

Figure 21. Periodic Loading and current intensity measured for: (a) a control specimen (without CNTs) at age of 35 d; (b) a self-sensing specimen with CNT grown fly ash at age of 35 d

3.4 Conclusions

In this chapter, we demonstrated that self-dispersing, geopolymeric nanocomposite can be successfully synthesized through directly growing CNTs on fly ash particles using the Poptube method. A few conclusions can be drawn based on this study.

1. Self-dispersing CNTs in the geopolymer matrix can be done by directing growing CNTs on fly ash particles using Poptube method. The difficult task of dispersing CNTs is eliminated.
2. The strength of the mortar samples can be slightly increased by the CNTs grown on the fly ash particles.

3. Raman spectra reveals that composite effect between the CNTs and the geopolymer matrix exists and the stress can be transferred from the geopolymer matrix to the CNTs.
4. Geopolymer mortar exhibits piezoresistivity at early age due to its high electric conductivity. However, severe polarized effect induced by the DC current is clearly observed. This polarized effect diminishes with age and becomes almost negligible at 35d.
5. The ability to sense the applied stress of the geopolymeric nanocomposite has been confirmed. Growing CNTs on fly ash makes the produced nanocomposite mortar three orders of magnitude more sensitive than without CNTs.

4. CONCLUSIONS AND FUTURE STUDY

4.1 Major Conclusions

CNT based nanocomposites are limited by the high cost and the difficulty of dispersing of the CNTs. The Poptube method used in this study may provide a viable solution to this problem. It not only eliminates the difficulty of dispersing the CNTs, but also significantly reduces the cost of the CNTs. The Poptube method requires very simple equipment and consumes little energy. The cost of CNTs obtained by this method is much lower than any other existing methods. In addition, it can be easily scaled up for large-scale manufacture. Based on this technique, next generation self-dispersing, self-sensing materials can be produced, which will immediately find their wide applications in many areas critically needed by our nation, such as energy, defense, and civil infrastructure systems.

In this study, a few key questions on using Poptube method to produce CNTs reinforced multifunctional geopolymeric nanocomposite are answered by experimental studies.

1. Growing CNTs have no adverse effect on the reactivity of fly ash in alkaline solution, as revealed by thermal conductivity testing. This is because the CNTs grown on the fly ash particles function as seeding site for the precipitation of geopolymerization.
2. AFM can be used to in-situ study the dissolution of fly ash and geopolymerization process. It has been shown that there exist preferred sites and direction for the dissolution of fly ash. The charges in both the solid and aqueous materials in fresh geopolymer are

3. high but reduce quickly with the formation of geopolymer which not only consumes the ions in the aqueous phases, but also covers the surface of solid phases.
4. Raman spectra can be used to measure the stress in CNTs. Stress in CNTs induced by temperature change can be clearly detected by Raman spectra. It has been revealed that the thermal stress in the CNTs is in proportion to the D-band shift.
5. At early age, geopolymer mortar is piezoresistive because of its high electric conductivity. However, DC induced polarization effect is very serious at this age. This polarization effect reduces with reaction time and becomes negligible at 35d.
6. Self-sensing geopolymeric nanocomposite can be produced by using fly ash grown with CNTs using Poptube method. Compared with the geopolymer mortar without CNTs, the produced nanocomposite is three orders magnitude more sensitive to the stress than the geopolymer one without any CNTs.

4.2 Suggestions for Future Study

This study explores the Poptube method to produce self-dispersing, self-sensing geopolymer nanocomposite. Although we successfully synthesized the nanocomposite, more work is needed to further refine this method.

1. Quality control of the CNTs grown on fly ash: In-situ growing CNTs on fly ash with Poptube method is ultra-fast and low-cost. As cost, the produced CNTs have poor quality and lack of consistence. As a result, the produced nanocomposite fails to achieve a significant improvement on mechanical strength. Future work is needed to improve the quality of the produced CNTs to achieve desired strength enhancement.

2. AFM is an excellent tool to in-situ examine the dissolution and geopolymerization of fly ash. This study revealed that the dissolution of fly ash left grooves on the surface of fly ash. This is a very interesting finding, and more study is needed to confirm it. All AFM study in this study was limited to plain fly ash. More work is needed to examine the fly ash grown with CNTs.
3. This study shows D-band of CNTs shift with stress in the CNT. This suggests that a non-contact method can be developed based on Raman spectra to measure the stress in CNT reinforced materials. More study shall be conducted to test this hypothesis.

5. REFERENCES

[1] "Mineral Commodity Summaries 2020," U.S. Geological Survey, Reston, 2020.

[2] "Inventory of U.S. Greenhouse Gas Emissions and Sinks," United States Environmental Protection Agency, 2020.

[3] "Technology Roadmap: Low-Carbon Transition in the Cement Industry. Geneva: World Business Council for Sustainable Development.," IEA, CSL & WBCSD, Geneva, 2018.

[4] "ASCE | 2017 Report Card for America's Infrastructure | Grade Sheet: Previous Grades," American Society of Civi lEngineers, 2017.

[5] P. Maravelaki-Kalaitzaki and G. Moraitou, "Sorel's cement mortars: Decay susceptibility and effect on Pentelic marble," *Cement and Concrete Research,* vol. 29, pp. 1929-1935, 1999.

[6] J. W. Harrison, "Reactive magnesium oxide cements". US Patent 0041785A1, 2003.

[7] L. Fernandez, C. Alonso, A. Hidalgo and Andrade, "The role of magnesium during the hydration of C3S and C-S-H formation. Scanning electron microscopy and mid-infrared studies," *Advanced Cement Research,* vol. 17, pp. 9-21, 2005.

[8] J. Paya, M. Borrachero, J. Monzo and M. Bonilla, "Properties of Portland cement mortars incorporating high amounts of oil-fuel ashes," *Waste Management,* vol. 19, no. 1, pp. 1-7, 1999.

[9] J. H. Sharp, C. D. Lawrence and R. Yang, "Delayed ettringite formation in heat-cured Portland cement. Adv. Cem. Res. 29, 17-25.," *Advanced Cement Research,* vol. 29, pp. 17-25, 1999.

[10] Zhang, F. P. Glasser and L., "High-performance cement matrices based on calcium sulphoaluminate-belite compositions," *Cement Concrete Research,* vol. 31, pp. 1881-1886, 2001.

[11] T. Grounds, D. V. Nowell and F. W. Wilburn, "Resistance of supersulfated cement to strong sulfate solutions," *Journal of Thermal Analysis and Calorimetry,* vol. 72, pp. 181-190, 2003.

[12] J. M. Roy and D. M., "The potential of fly ash for cement manufacture," *American Ceramic Society Bulletin; (United States),* vol. 72, pp. 77-81, 1993.

[13] P. Arjunan, M. R. Silsbee and D. M. Roy, "Sulphoaluminate–belite cement from low-calcium fly ash and sulfur-rich and other industrial byproducts," *Cement Concrete Research,* vol. 29, pp. 1305-1311, 1999.

[14] B. K. Day and M. R. L., "Pozzolanic and cementitious reactions of fly ash in blended cement pastes," *Cement Concrete Research,* vol. 18, pp. 301-310, 1988.

[15] R. Brough, C. M. Dobson, I. G. Richardson and G. W. Groves, "A study of the pozzolanic reaction by solid-state 29Si nuclear magnetic resonance using selective isotopic enrichment," *Journal of Materials Science,* vol. 30, pp. 1671-1678, 1995.

[16] J. Davidovits, "Geopolymer Chemistry and Properties," in *Geopolymer '88, First European Conference on Soft Mineralurgy*, Compiegne, France, 1988.

[17] J. Davidovits, "Synthetic Mineral Polymer Compound of The Silicoaluminates Family and Preparation Process". US Patent 4,472, 1984.

[18] J. Davidovits, "Properties of Geopolymer Cements," in *In Kiev (Ed.), First International Conference on Alkaline Cements and Concretes*, Kiev, Ukraine, Kiev State Technical University, 1994, pp. 131-149.

[19] J. Davidovits, "Chemistry of Geopolymeric Systems,Terminology," in *Geopolymere '99 International Conference*, Saint-Quentin, France, 1999.

[20] J. Davidovits, "High-Alkali Cements for 21st Century Concretes," in *V. Mohan Malhotra Symposium on Concrete Technology: Past, Present And Future*, University of California, Berkeley, 1994.

[21] D. Roy, "Alkali-activated cements—opportunities and challenges," *Cement Concrete Research,* vol. 29, pp. 249-254, 1999.

[22] A. Palomo and J. L. d. Fuente, "Alkali-activated cementitous materials: Alternative matrices for the immobilisation of hazardous wastes: Part I. Stabilisation of boron," *Cement and Concrete Research,* vol. 33, no. 2, pp. 281-288, 2003.

[23] P. Duxson, A. Fernández-Jiménez, J. Provis, G. Lukey, A. Palomo and J. V. Deventer, "Geopolymer technology: the current state of the art," *Journal of Materials Science,* vol. 42, pp. 2917-2933, 2007.

[24] R. Lloyd, J. Provis and J. van Deventer, "Microscopy and microanalysis of inorganic polymer cements. 1: Remnant fly ash particles," *ournal of Materials Science,* vol. 44, pp. 608-619, 2009.

[25] R. Lloyd, J. Provis and J. van Deventer, "Microscopy and microanalysis of inorganic polymer cements. 2: The gel binder," *Journal of Materials Science,* vol. 44, pp. 620-631, 2009.

[26] D. D. Siemer, "Hydroceramics, a "new" cementitious waste form material for US defense-type reprocessing waste," *Materials Research Innovations,* vol. 6, pp. 96-104, 2002.

[27] K. Zaharaki and K. Dimitra, "Geopolymerisation: A review and prospects for the minerals industry," *Mineral Engineering,* vol. 20, pp. 1261-1227, 2007.

[28] Deventer, H. Xu and J. Van, "The geopolymerisation of alumino-silicate minerals," *International Journal of Mineral Processing,* vol. 59, p. 247–266, 2000.

[29] V. B. Mackenzie and K.J.D., "Synthesis and thermal behaviour of potassium sialate geopolymers," *Materials Letters,* vol. 57, p. 1477–1482, 2003.

[30] V. B. Mackenzie and K.J.D., "Thermal behaviour of inorganic geopolymers and composites derived from sodium polysialate," *Materials Research Bulletin,* vol. 38, p. 319–331, 2003.

[31] R. Cioffi, L. Maffucci and L. Santoro, "Optimization of geopolymers synthesis by calcinations and polycondensation of a kaolinitic residue," *Resources Conservation and Recycling,* vol. 40, pp. 27-38, 2003.

[32] P. Krivenko and J. Skurchinskaya, in *International Conference on the Utilization of Fly Ash and Other Coal Combustion By-products*, Shanghai, 1991.

[33] A. Palomo, M. Grutzeck and M. Blanco, "Alkali-activated fly ashes – A cement for the future," *Cement and Concrete Research,* vol. 29, p. 1323–1329, 1999.

[34] Phair and J.W., "Compositional effects and microstructure of fly ash-based geopolymers," *PhD Thesis, Department of Chemical Engineering, University of Melbourne, Victoria, Australia,* 2001.

[35] J. Phair, J. V. Deventer and J. Smith, "Mechanism of polysialation in the incorporation of zirconia into fly ash-based geopolymers," *Industrial and Engineering Chemistry Research,* vol. 39, p. 2925–2934, 2000.

[36] B. Rangan, D. Hardjito, S. Wallah and D. Sumajouw, "Studies on fly ash-based geopolymer concrete," in *Davidovits, J. (Ed.), Proceedings of the World Congress Geopolymer,* Saint Quentin, France, 2005.

[37] J. Strydom, Swanepoel and C.A., "Utilisation of fly ash in a geopolymeric material," *Applied Geochemistry,* vol. 17, p. 1143–1148, 2002.

[38] V. Jaarsveld and J.G.S., "The physical and chemical characterisation of fly ash based geopolymers," *PhD Thesis, Department of Chemical Engineering, University of Melbourne, Australia,* 2000.

[39] J. J.G.S., J. Van Deventer, Van and G. Lukey, "The characterisation of source materials in fly ash-based geopolymers," *Materials Letters,* vol. 57, p. 1272–1280, 2003.

[40] C. Yip, V. Deventer and J.S.J., "Effect of granulated blast furnace slag on geopolymerisation," in *6th World Congress of Chemical Engineering Melbourne*, Australia, 2001.

[41] C. Yip, G. Lukey and J. V. Deventer, "Effect of blast furnace slag addition on microstructure and properties of metakaolinite geopolymeric materials," *Ceramic Transactions,* vol. 153, p. 187–209, 2004.

[42] D. Zaharaki, K. Komnitsas and V. Perdikatsis, "Factors affecting synthesis of ferronickel slag based geopolymers," in *2nd International Conference on Advances in Mineral Resources Management and Environmental Geotechnology*, Chania, Crete, Greece, 2006.

[43] K. Komnitsas, D. Zaharaki and V. Perdikatsis, "Geopolymerisation of low calcium ferronickel slags," *Journal of Materials Science,* vol. 42, p. 3073–3082, 2007.

[44] K. Goretta, N. Chen, F. Gutierrez-Mora, J. Routbort, G. Lukey and J. V. Deventer, "Solid-particle erosion of a geopolymer containing fly ash and blast-furnace slag," *Wear,* vol. 256, p. 714–719, 2004.

[45] T. C. Chiu and J.P., "Fire-resistant geopolymer produced by granulated blast furnace slag," *Minerals Engineering,* vol. 16, p. 205–210, 2003.

[46] S. Astutiningsih and Y. Liu, "Geopolymerisation of Australian slag with effective dissolution by the alkali," in *World Congress Geopolymer*, Saint Quentin, France, 2005.

[47] P. Duxson, J. Provis, G. Lukey and J. v. Deventer, "The role of inorganic polymer technology in the development of 'Green concrete'," *Cement Concrete Research,* vol. 37, p. 1590–1597, 2007.

[48] A. C. A. Association, "CCP production and use survey results (revised)," 2007. [Online]. Available: http://www.acaa_usa.org.

[49] K. Scrivener and R. Kirkpatrick, "Innovation in use and research on cementitious material," *Cement and Concrete Research,* vol. 38, pp. 128-136, 2008.

[50] Malhotra and V.M., "High-performance high-volume fly ash concrete," *Concrete International,* vol. 24, pp. 1-5, 2002.

[51] J. Phair, "Green chemistry for sustainable cement production and use," *Green Chemistry,* vol. 8, pp. 763-780, 2006.

[52] D. Khale and R. Chaudhary, "Mechanism of geopolymerization and factors influencing its development: a review," *Journal of Material Science,* vol. 42, pp. 729-746, 2007.

[53] C. Bakis, L. Bank, V. Brown, M.ASCE, E. Cosenza, J. F. Davalos, J. J. Lesko, A. Machida, S. H. Rizkalla and T. Triantafillou, "Fiber-Reinforced Polymer Composites for Construction—State-of-the-Art Review," *Journal of Composites for Construction,* vol. 6, pp. 73-87, 2002.

[54] E. a. E. M. R. Saadatmanseh, "Application of Fibre-Composites in Civil Engineering," in *7th ASCE Structures Congress,* 1989.

[55] A. C. 440, "Design and Construction of Externally Bonded FRP Systems for Strengthening Concrete Structures (ACI 440.2R-02)," American Concrete Institute, Farmington Hills, MI, 2002.

[56] V. M. Karbhari, J. W. Chin, D. Hunston, B. Benmokrane, T. Juska, M. Morgan, J. J. Lesko, U. Sorathia and D. Reynaud, "Durability Gap Analysis for Fiber-Reinforced Polymer Composites in Civil Infrastructure," *Journal of Composites for Construction,* vol. 7, pp. 238-247, 2003.

[57] M. Porter and K. Harries, "Workshop on Research in FRP Composites in Concrete Construction," Final Report Submitted to NSF, 2005.

[58] H. JA, B. PN and L. RE, "Strength retention of fire-resistant aluminosilicate-carbon composites under wet-dry conditions," *Composites Part B: Engineering,* vol. 31, pp. 107-111, 2000.

[59] L. RE, B. PN, F. A, S. U, D. J and D. M, "Fire-resistant Aluminosilicate Composites," *Fire And Meterials,* vol. 21, pp. 67-73, 1997.

[60] Q. Balaguru, Z. B., N. T. and R. P., "Novel geopolymer based composites with enhanced ductility," *Journal of Material Science,* vol. 42, pp. 3131-3137, 2007.

[61] C. Papakonstantinou and P. Balaguru, "Bond characteristics and structural behavior of inorganic polymer FRP," *Measuring, Monitoring and Modeling Concrete Properties,* pp. 735-741, 2006.

[62] A. Ferna´ndez-Jime´nez and A. Palomo, "Characterisation of fly ashes. Potential reactivity as alkaline cements," *Fuel,* vol. 82, p. 2259–2265, 2003.

[63] B. Jha and D. N. Singh, Fly Ash Zeolites, 8210 Aarhus, V-DK, Denmark: Chemistry and Materials Science, 2016.

[64] J. S. J. Sindhunata, v. Deventer, G. C. Lukey and H. Xu, "Effect of Curing Temperature and Silicate Concentration on Fly-Ash-Based Geopolymerization," *Industrial & Engineering Chemistry Research,* vol. 45, no. 10, p. 3559–3568, 2006.

[65] K. S., K. R., A. T.C., B. A. S.P. and Mehrotra, "Effects of Mechanically Activated Fly ash on the Properties of Geoplymer Cement," in *World Congress Geopolymer 2005*, 2005.

[66] M. Yu, B. Files, S. Arepalli and a. R. Ruoff, "Tensile loading of ropes of single wall carbon nanotubes and their mechanical properties," *Physical Review Letter,* vol. 84, p. 5552, 2000.

[67] P. Calvert, "Strength in disunity," *Nature,* vol. 357, p. 365–366, 1992.

[68] R. Ruoff and D. Lorents, "Mechanical and thermal properties of carbon nanotubes," *Carbon,* vol. 33, pp. 925-930, 1995.

[69] S. Iijima, C. Brabec and A. B. Z. Maiti, "Structural flexibility of carbon nanotubes," *The Journal of Chemical Physics,* vol. 104, p. 2089–2092, 1996.

[70] M. Treacy, T. Ebbesen and J. Gibson, "Exceptionally high Young's modulus observed for individual carbon nanotubes," *Nature,* vol. 381, p. 678–680, 1996.

[71] M. e. a. Falvo, "Bending and buckling of carbon nanotubes under large strain," *Nature,* vol. 389, p. 582–584, 1997.

[72] D. MS, D. G, C. JC and H. E., "Electronic, Thermal and Mechanical Properties of Carbon Nanotubes," *Philosophy Transactions of the Royal Society of London A,* vol. 362, p. 2065–2098, 2004.

[73] S. Subramooney, "Nanocarbons—structure, properties, and potential applications," *Advanced Materials,* vol. 15, pp. 1157-1475, 1998.

[74] I. Kang, M. J. Schulz, J. H. Kim, V. Shanov and D. Shi, "A carbon nanotube strain sensor for structural health monitoring," *Smart Mater. Struct,* vol. 15, pp. 737-748, 2006.

[75] X. Yu, "Development of carbon-nanotube/cement composite for traffic flow detection. Seed project final report," Northland Advanced Transportation Systems Research Laboratories, 2009.

[76] E. T. Thostenson and T.-W. Chou, "Carbon nanotube networks: sensing of distributed strain and damage for life prediction and self-healing," *Advanced Materials,* vol. 19, pp. 2837-2841, 2006.

[77] E. Thostenson and T.-W. Chou, "Real-time in situ sensing of damage evolution in advanced fiber composites using carbon nanotube networks," *Nanotechnology*, vol. 19, p. 215713, 2008.

[78] S. Shah, M. Konsta-Gdoutos, Z. Metaxa and P. Mondal, "Nanoscale Modification of Cementitious Materials," *Nanotechnology in Construction*, vol. 3, pp. 125-130, 2009.

[79] J. Makar and J. Beaudoin, "Carbon nanotubes and their applications in the construction industry," in *1st International Symposium on Nanotechnology in Construction*, Royal Society of Chemistry, 2004.

[80] G. Li, P. Wang and X. Zhao, "Mechanical behavior and microstructure of cement composites incorporating surface-treated multi-walled carbon nanotubes," *Carbon*, vol. 43, p. 1239–1245, 2005.

[81] J. Makar, J. Margeson and J. Luh, "Carbon nanotube/cement composites – Early results and potential applications," in *3rd International Conference on Construction Materials: Performance, Innovations and Structural Implications*, Vancouver, Canada, 2005.

[82] G. Li, P. Wang and X. Zhao, "Pressure-sensitive and microstructure of carbon nanotube reinforced cement composites," *Cement and Concrete Composites*, vol. 29, p. 377–382, 2007.

[83] Y. Saez de Ibarra, J. Gaitero, E. Erkizia and I. Campillo, "Atomic force microscopy and nanoindentation of cement pastes with nanotube dispersions," *Physica Status Solidi (a)*, vol. 203, p. 1076–1081, 2006.

[84] S. Wansom, N. Kidner, L. Woo and T. Mason, "AC-impedance response of multiwalled carbon nanotube/cement composites," *Cement and Concrete Composites*, vol. 28, p. 509–519, 2006.

[85] A. Cwirzen, K. Habermehl-Chirzen and V. Penttala, "Surface decoration of carbon nanotubes and mechanical properties of cement/carbon nanotube composites," *Advanced Cement Research*, vol. 20, pp. 65-73, 2008.

[86] F. Sanchez and C. Ince, "Microstructure and macroscopic properties of hybrid carbon nanofiber/silica fume cement composites," *Composites Science and Technology*, vol. 69, pp. 1310-1318, 2009.

[87] F. Sanchez, L. Zhang and C. Ince, "Multi-scale Performance and Durability of Carbon Nanofiber/Cement Composites," *Nanotechnology in Construction*, vol. 3, pp. 345-350, 2009.

[88] S. F. and S. K., "Nanotechnology in concrete- A review," *Construction and Building Materials*, vol. 24, pp. 2060-2071, 2010.

[89] X. L. Xie, Y. Mai and X. Zhou, "Dispersion and alignment of carbon nanotubes in polymer matrix: a review," *Materials Science and Engineering: R: Reports,* vol. 49, pp. 89-112, 2005.

[90] J.-P. Salvetat, G. Briggs, J.-M. Bonard and R. B. a. A. Kulik, "Elastic and Shear Moduli of Single-Walled Carbon Nanotube Ropes," *Physical Review Letters,* vol. 82, pp. 944-947, 1999.

[91] M. Sennett, E. Welsh, J. Wright, W. Li, J. Wen and J. Ren, "Dispersion and Alignment of Carbon Nanotubes in Polycarbonate," *Applied Physics A: Materials Science & Processing,* vol. 76, pp. 111-113, 2003.

[92] R. Haggenmueller, H. Gommans, A. Rinzler, J. Fischer and K. Winey, "Aligned Single-wall Carbon Nanotubes in Composites by Melt Processing Methods," *Chemical Physics Letters,* vol. 330, no. 3-4, p. 219–225, 2000.

[93] R. Andrews and M. Weisenberger, "Carbon Nanotube Polymer Composites," *Current Opinion In Solid State & Materials Science,* vol. 8, no. 1, p. 31–37, 2004.

[94] W. Dondero and R. Gorga, "Morphological and Mechanical Properties of Carbon Nanotube/Polymer Composites via Melt Compounding," *Journal of Polymer Science Part B Polymer Physics,* vol. 44, no. 5, pp. 864-878, 2006.

[95] N. AG, S. SD, N. LI, C. A, M. PR, C. KH and e. al., "A novel cement-based hybrid material," *New Journal of Physics,* vol. 11, 2009.

[96] Z. Liu, J. Wang, V. Kushvaha, S. Poyraz, H. Tippur, S. Park, M. Kim, Y. Liu, J. Bar, H. Chen and X. Zhang, "Poptube approach for ultrafast carbon nanotube growth," *Chemical Communications,* vol. 47, no. 35, pp. 9912-9914, 2011.

[97] P. SH, K. C, J. YI, L. DY, L. YE and Y. KS., "Activation behaviors of isotropic pitch-based carbon fibers from electrospinning and meltspinning," *Synthetic Metals,* vol. 146, pp. 207-212, 2004.

[98] C. G, L. BB, M. CR, F. ER and R. RS., "Chemical vapor deposition based synthesis of carbon nanotubes and CNTs using a template method," *Chem. Mater.,* vol. 10, pp. 260-267, 1998.

[99] K. M, D. B, C. EB, K. T, J. M and M. K., "Synthesis of mesoporous carbons using ordered and disordered mesoporous silica templates and polyacrylonitrile as carbon precursor," *J. Phys. Chem. B,* vol. 109, pp. 9216-9225, 2005.

[100] Zeng X and W. J., "Characterization of mechanical and electric properties of geopolymers synthesized using four locally available fly ashes," *Construction and Building Materials,* vol. 121, pp. 386-399, 2016.

[101] L. MP, M. F and S. J., "Rapid evaluation of pozzolanic activity of natural products by conductivity measurements," *Cem. Concr. Res.*, vol. 19, pp. 63-68, 1989.

[102] W. HD and V. RA., "Nanocomposites: issues at the interface," *Materials Today,* vol. 7, pp. 38-42, 2004.

[103] C. SN, C. RA, B. RE and P. MS, "Raman spectroscopy for characterization of interfacial debonds between carbon fibers and polymer matrices," *Composite Structures,* vol. 76, pp. 375-387, 2006.

[104] S. LS, G. SC and A. PM., "Load transfer in carbon nanotubes epoxy composites," *Appl. Phys. Lett.*, vol. 73, pp. 3842-3844, 1998.

[105] A. PM, S. LS, G. C and R. A., "Single-walled carbon nanotube-polymer composites: strength and weakness," *Adv. Mater.*, vol. 12, pp. 750-753, 2000.

[106] Zhao Q and W. HD., "Raman spectroscopy of carbon-nanotube-based composites," *Phil. Trans. R. Soc. Lond. A,* vol. 362, pp. 2407-2424, 2004.

[107] L. O and W. HD., "Evaluation of Young's modulus of carbon nanotubes by micro- Raman spectroscopy," *J. Mater. Res.*, vol. 13, pp. 2418-2422, 1998.

[108] S. Zeng and J. Wang, "Characterization of mechanical and electric properties of geopolymers synthesized using four locally available fly ashes," *Construction and building materials,* vol. 121, pp. 386-399, 2016.

[109] S. Sasmal, N. Ravivarman and B. Sindu, "Synthesis, characterisation and performance of piezo-resistive cementitious nanocomposites," *Cement and Concrete Composites,* Vols. 10-21, p. 75, 2017.

[110] "4. Industrial Processes," U.S. Environmental Protection Agency, Washington, DC, 2017.